FACULTY OF SCIENCE AND TECHNOLOGY

MASTER'S THESIS

Study programme / specialisation: Biological Chemistry	The spring semester, 2023 Open access
Author: Mathilde Nystuen Servan	
Supervisor at UiS: Cato Brede External supervisor(s): Grete Jonsson	
Thesis title: Exploring potential analytical methods for determination of glycerol-3-phosphate in human plasma	
Credits (ECTS): 60 p	
Keywords: G3P, Derivatization, HPLC-F, LC-MS, HILIC, Chronic kidney disease	Pages: 52 + appendix: 3 Stavanger, *(15.08.2023)*

Abstract

Chronic kidney disease (CKD) is a progressive condition where the kidneys gradually lose their ability to function properly. Biomarkers that indicate immediate renal tissue injury is needed for improved detection of early CKD. One potential biomarker is glycerol-3-phosphate (G3P), a small organic ion which recently has been inked to kidney injury through regulation of fibroblast growth factor 23 (FGF23). The aim of this study was to explore potential analytical methods for determination of G3P in human plasma. G3P was retained and analyzed on a hydrophilic interaction liquid chromatography (HILIC) column using liquid chromatography-mass spectrometry (LC-MS). Further, derivatization with alcohols through an esterification reaction was possible, which offered retention using reversed phase (RP) LC. However, the reaction conditions potentially lead to phospholipid hydrolysis, which increased the amount of G3P. Further research could explore the possibilities of phospholipid extraction through liquid-liquid extraction (LLE) or solid phase extraction (SPE).

Acknowledgements

I would like to take this opportunity to express my heartfelt appreciation to those who have supported and guided me throughout my master's thesis journey.

First and foremost, my sincere gratitude to my supervisors for trusting me with this interesting, and challenging, project. I am grateful for my supervisor Cato Brede's enthusiasm and creativity, which have truly been a source of inspiration. I would like to thank my supervisor Grete Jonsson for her invaluable guidance and insightful feedback.

I am also grateful to the department of Medical Biochemistry at Stavanger University Hospital (SUS), for letting me access their excellent facilities and resources.

Finally, I am grateful to my family and friends for their encouragement and belief in my abilities. I would like to extend a profound note of gratitude to my father for taking care of my daughter during my work.

Stavanger, August 2023

Mathilde Nystuen Servan

Contents

ABSTRACT ..... **II**

ACKNOWLEDGEMENTS ..... **III**

ABBREVIATIONS ..... **VI**

1 INTRODUCTION **1**

2 THEORY **4**

2.1 GLYCEROL-3-PHOSPHATE 4

2.2 LIQUID CHROMATOGRAPHY 5

2.2.1 Columns *7*

2.2.1.1 Normal-phase chromatography 7

2.2.1.2 Reversed phase chromatography 7

2.2.1.3 Hydrophilic interaction liquid chromatography 8

2.2.2 Detection *9*

2.2.2.1 Fluorescence spectroscopy 10

2.2.2.2 Mass spectrometry 11

2.3 SAMPLE PREPARATION 15

2.3.1 Sample collection and storage *15*

2.3.2 Extraction *16*

2.3.3 Protein precipitation *17*

2.3.3 Derivatization *17*

2.4 DERIVATIZATION OF G3P 18

3 EXPERIMENTAL **21**

3.1 CHEMICALS AND EQUIPMENT 21

3.1.1 Chemicals *21*

3.1.2 Equipment *21*

3.2 DERIVATIZATION PROCEDURES 22

3.2.1 Preliminary evaluation of fluorescent derivatization reagents *22*

3.2.2 Derivatization with 9-fluorenemethanol *23*

3.2.3 Derivatization with butanol *25*

3.3 ANALYSIS OF G3P USING HILIC 26

3.3.1 Simplex optimization *26*

3.3.2 Variation of measured G3P between days *27*

3.4 SAMPLE PREPARATION AND G3P EXTRACTION 27

3.5 THE EFFECT OF HEAT AND ACID ON G3P AMOUNT IN PLASMA 28

4 RESULTS **29**

4.1 DERIVATIZATION OF G3P 29

4.1.1 Preliminary evaluation of fluorescent derivatization reagents *29*

4.1.2 Derivatization with 9FlMe *29*
4.1.3 Derivatization with butanol *31*
4.2 Analysis of G3P using HILIC 32
4.2.1 Simplex optimization *34*
4.2.2 Variation of measured G3P between days *35*
4.3 Sample preparation and G3P extraction 35
4.4 The effect of heat and acid on G3P amount in plasma 36

5 DISCUSSION 38

5.1 Derivatization 38
5.2 HILIC 38
5.3 Phospholipid hydrolysis 39
5.4 Conclusion 40

REFERENCES 41

APPENDIX I 46

APPENDIX II 47

Abbreviations

Abbreviation	Explanation
1NaMe	1-Naphtalenemethanol
9AnMe	9-Anthracenemethanol
9FlMe	9-Fluorenemethanol
ACN	Acetonitrile
AKI	Acute kidney injury
ATP	Adenosine triphosphate
BuOH	Butan-1-ol
CKD	Chronic kidney disease
EDTA	ethylenediaminetetraacetic acid
eGFR	estimated glomerular filtration rate
ESI	Electrospray ionization
EtOH	Ethanol
F	Fluorescence detector
FGF23	Fibroblast growth factor 23
G3P	Glycerol-3-phosphate
GPAT	Glycerol-3-phosphate acyltransferase
HCl	Hydrochloric acid
HILIC	Hydrophilic interaction liquid chromatography
HPLC	High performance liquid chromatography
LC	Liquid chromatography
LLE	Liquid-liquid extraction
LOD	Limit of detection
LPA	Lysophosphatidic acid
m/z	Mass to charge
MeOH	Methanol
MRM	Multiple reaction monitoring
MS	Mass spectrometry
NP	Normal phase
PBS	Phosphate buffer saline
PPT	Protein precipitation

PrOH	Propanol
PTSA	p-toluenesulfonic acid
RP	Reverse phase
SD	Standard deviation
SPE	Solid phase extraction
TOF	Time of flight
UPLC	Ultra performance liquid chromatography
UV-vis	Ultraviolet-Visible

1 Introduction

The kidneys play a crucial role in filtering waste and excess fluids from the blood, maintaining electrolyte balance, and producing hormones that regulate blood pressure and stimulate red blood cell production. Chronic kidney disease (CKD) is a progressive condition where the kidneys gradually lose their ability to function properly. At least 10 % of adults worldwide suffer from CKD and its growing prevalence is a global health concern (Kalantar-Zadeh et al., 2021; Lv & Zhang, 2019)**.** CKD can be a result of underlying health conditions which cause damage to the kidneys over time, such as diabetes, glomerulonephritis, and cystic kidney diseases. Risk factors include high blood pressure, smoking, inactivity, and obesity. Early stages of CKD have no symptoms, which is why routine screening tests are important for early detection. Its progression can be managed through lifestyle changes, medication and in more advanced cases, dialysis, or kidney transplantation. The progression of CKD is measured from the estimated glomerular filtration rate (eGFR), where 60 ml per minute per 1.73 m^2 is defined as CKD. eGFR is calculated based on the levels of creatinine (waste product) in the blood along with factors such as age, sex, and race. The main limitation with this method is inaccuracy in determining early CKD in individuals compared to groups (Alaini et al., 2017). The rate of creatinine production and elimination can differ greatly between individuals, due to lifestyle factors such as diet and exercise. Furthermore, when eGFR is low, it is often too late for preventive measures. Biomarkers which indicate immediate injury of the renal tissue can improve early detection of CKD.

One potential biomarker is glycerol-3-phosphate (G3P), a small organic ion which recently has been inked to kidney injury (Simic et al., 2020). The role of G3P in this context is regulation of fibroblast growth hormone 23 (FGF23). FGF23 is a hormone produced by osteocytes in bone tissue, and its main function is to regulate phosphate reabsorption and decrease vitamin D production (Liu & Quarles, 2007). FGF23 maintains phosphate homeostasis and prevents excessive accumulation of phosphate in the blood by reducing phosphate reabsorption from the renal tubules into the bloodstream. FGF23 indirectly lowers vitamin D levels by suppressing the production of 1-alpha-hydroxylase in the kidneys, which is responsible for converting inactive vitamin D into its active form (Martin et al., 2012). Since the main target for FGF23 is the kidney, elevated FGF23 levels is strongly associated with CKD (Wahl & Wolf, 2012) Simic et al. (2020) demonstrated how G3P derived from the injured kidney regulates FGF23 production through lysohosphatidic acid (LPA) synthesis in

bone marrow (**Figure 1**). G3P is synthesized to LPA by G3P acyltransferases (GPATs). LPA functions as a signal molecule which binds to the receptor LPAR1. Binding of LPA to LPAR1 then stimulates FGF23 production. Mice administered G3P showed increased levels of FGF23 and lowered phosphate levels in blood plasma. Further, mice and humans with acute kidney injury (AKI) rapidly showed elevated levels of G3P in blood in a study using liquid chromatography-mass spectrometry (LC-MS) based metabolomics, where G3P was one out of 1600 detected molecules (Simic et al., 2020). The study participants included in this research had an average eGFR of 66.6 ml/min per 1.73 m^2, along with hypertension and other risk factors for kidney disease. Currently, it remains unclear whether healthy individuals exhibit any detectable levels of circulating G3P.

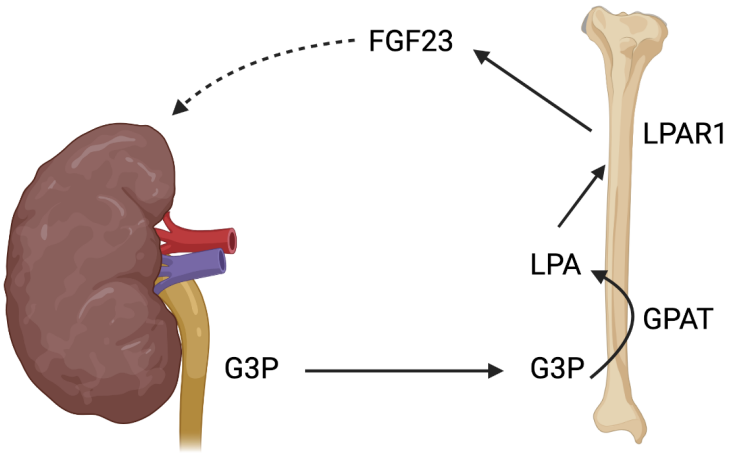

Figure 1. G3P derived from the injured kidney regulates the production of FGF23 through G3P GPAT-mediated LPA synthesis. LPAR1 mediates the effect of G3P and LPA on FGF23 production. Figure adapted from Simic et al. (2020).

Previously, G3P from blood samples have been analyzed using hydrophilic interaction liquid chromatography, however no concentrations have been reported (Chiles et al., 2019; Simic et al., 2020). In addition, assay kits are available that utilizes an enzymatic reaction producing a colorimetric or fluorescent product detectable with ultraviolet-visible (UV-Vis) or fluorescence spectrophotometry. Assay kits are for research only, and not intended for diagnostics, as reported by the manufacturers G3P-kits (Abcam, 2023).

The objective of this thesis was to explore potential analytical methods for G3P in human plasma or serum samples. Initially, the aim was to establish a sensitive analysis method using reversed phase (RP) high performance liquid chromatography coupled with a

fluorescence detector (HPLC-F). Since G3P is a small polar ion with no fluorophore, derivatization was necessary to achieve retention on reverse phase columns and fluorescence detection. Preliminary testing revealed that esterification with an alcohol was possible, prompting further investigation of this method.

2 Theory

2.1 Glycerol-3-phosphate

G3P is a small intermediate compound that plays a key role in several metabolic pathways, particularly in the breakdown and synthesis of lipids (Lee & Ridgway, 2020). It is derived from glycerol, a three-carbon molecule, through phosphorylation by glycerol kinase (**Figure 2a**) (Thorner & Paulus, 1973). G3P can also originate from dihydroxyacetone phosphate, an intermediate in glycolysis, catalyzed by cytosolic glycerol-3-phosphate dehydrogenase (**Figure 2b**). If glucose levels are low, G3P can also be synthesized from metabolites originating from the citric acid cycle, such as pyruvate or lactate, through the glyceroneogenesis pathway (Reshef et al., 2003). This pathway regulates lipid generation and takes place in adipose tissue and the liver.

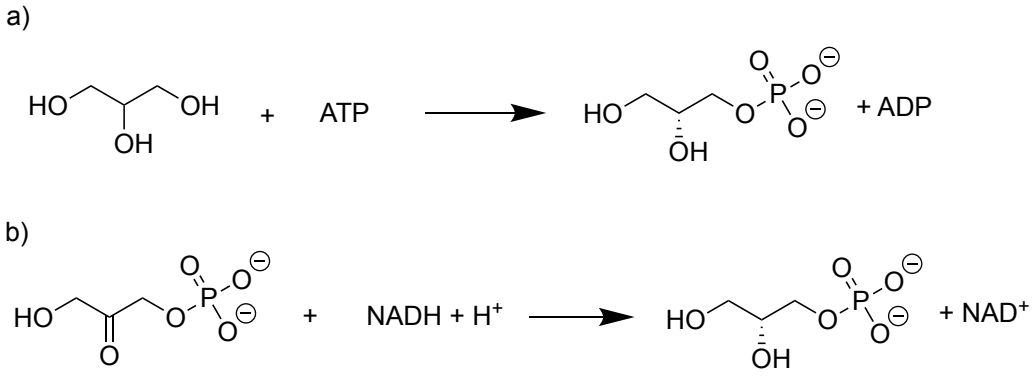

Figure 2. Synthesis of glycerol-3-phosphate from a) glycerol and adenosine triphosphate (ATP) or b) dihydroxyacetone phosphate and nicotinamide adenine dinucleotide + hydrogen (NADH).

G3P serves as a precursor for the synthesis of triglycerides, the main storage form of dietary fats. Additionally, G3P is involved in the synthesis of phospholipids, the major components of cell membranes. Phosphatidic acid, a precursor for the synthesis of phospholipids, is produced by successive acylation of G3P by glycerol-3-phosphate acyltransferases. Phosphatidic acid can be synthesized to phosphatidylglycerol and phosphatidylcholine which is found in relatively low and high amounts in mammalian cells, respectively (Tijburg et al., 1989).

G3P has recently been associated with kidney injury, where it is thought to be an FGF23 regulator (Simic et al., 2020). G3P was thought to be synthesized as a response to restricted blood flow to the kidneys (ischemia) and is transported through the blood stream to bone marrow. It is not known whether G3P levels in blood will increase due to ischemia in other organs as well, or if it is specific to kidney injury.

G3P is a hydrophilic ion containing two hydroxyl groups and one phosphate group. At normal blood pH (~7.4), the phosphate group is fully deprotonated (pK_{a1} 2.14 and pK_{a2} 7.2 for phosphoric acids), resulting in a net charge of -2. The relatively low mass, negative charge, and hydrogen bonding abilities, results in a high solubility in water. Estimates by EPI Suite™ software suggests it is possible to dissolve as much as 1 000 g/L of G3P in water. The estimated octanol-water partition coefficient K_{ow} is only 0.01, which indicates a low solubility in non-polar solvents. Further, there is no chromophore in the molecule, hence it will not absorb light nor possess fluorescence.

2.2 Liquid chromatography

Liquid chromatography (LC) is an analytical technique that separates and analyzes components of a mixture based on their differential interactions with a stationary phase and a mobile phase (Snyder et al., 2010). The sample mixture is dissolved and carried in a solvent mobile phase through the stationary phase. The stationary phase is located on the surface of porous particles in a packed column. It can either be the surface of a material like silica or a polymer, or it can take the form of a bonded phase containing a specific functional group. As the mobile phase passes through the column, the individual components of the sample interact differently with the stationary phase based on factors such as polarity, charge, size, and affinity. These interactions cause the components to partition differently between the stationary and mobile phase, and thus separate from each other and move at different rates through the column.

The LC-instrumentation setup consists of a mobile phase reservoir, a pump, an injector/autosampler, a column, a detector, and data acquisition system (**Figure 3**). The mobile phase is stored in a reservoir and often consists of water and an organic solvent. The mobile phase composition can be adjusted throughout the analysis or kept constant (gradient or isocratic elution). Dual reciprocating pumps delivers the mobile phase from the reservoir to the column at a specific flow rate throughout the analysis. The injector or autosampler introduces the sample into the chromatographic system. The column contains the stationary phase, which may vary depending on the specific chromatographic technique, and is often placed in an oven or heater used to control the temperature. The detector monitors the eluted analytes from the column and generates a signal which represents their concentration or presence. The individual components can be detected using methods such as ultraviolet-

visible (UV-Vis) spectroscopy, fluorescence spectroscopy, or mass spectrometry. The data acquisition system collects the signals generated by the detector, which can be viewed and processed in a computer software.

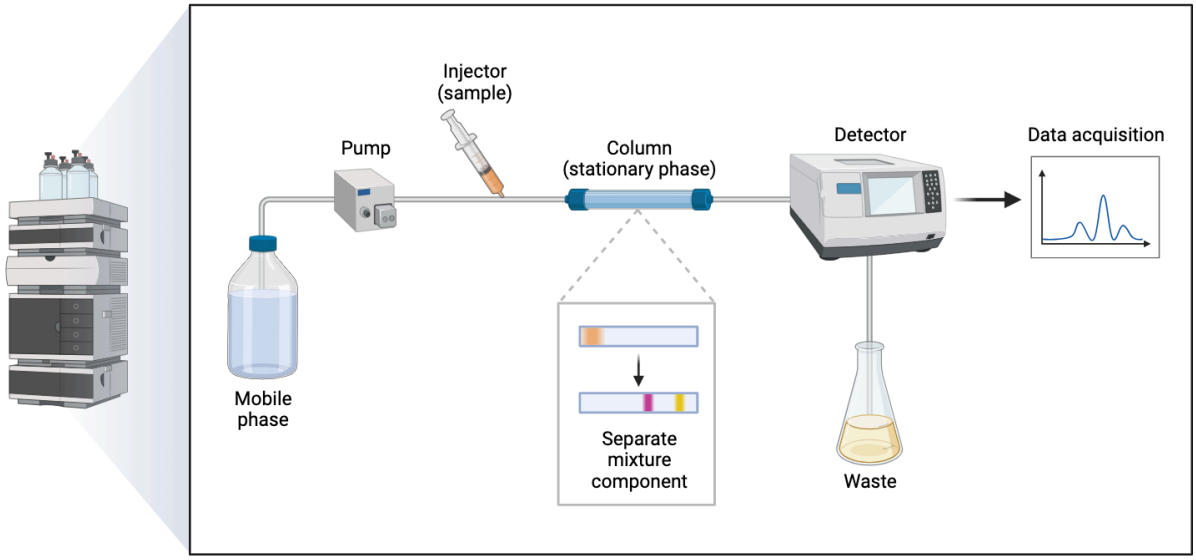

Figure 3. LC instrumentation setup. The mobile phase is delivered to the stationary phase located inside the column using a pump. The mixture components are separated in the column due to different interaction with the stationary phase. Once eluted from the column, the detector can register and/or quantify the analytes, and the output can be interpreted using a computer software.

The output is a chromatogram, a graphical representation of the chromatographic separation (**Figure 4**). It is a plot of the response from the detector (e.g. signal intensity) against time, illustrating the elution profile of analytes in the sample. A chromatogram consists of peaks corresponding to individual analytes in the sample. The position of each peak along the axis represents the retention time, which is the time taken for an analyte to reach the detector after injection. The height or area of each peak corresponds to the concentration of the analyte present in the sample. Components can be identified by comparing the retention time to known standards, in addition to analyzing the output from the detector. Furthermore, the peak area or height can be utilized for quantification purposes, providing a measure of the analyte's concentration.

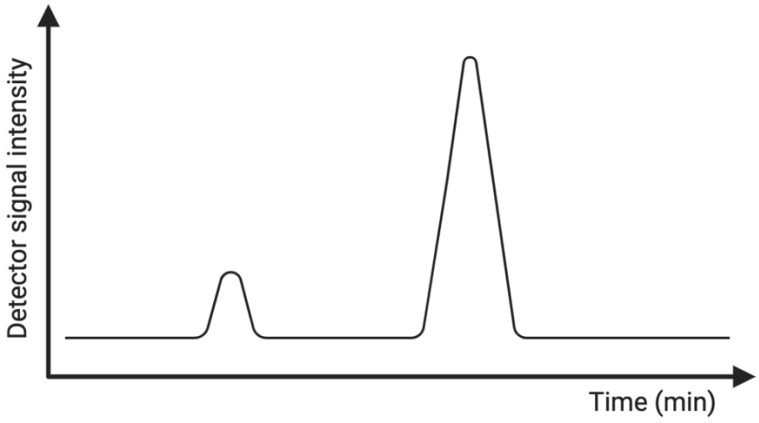

Figure 4. Example of a chromatogram with two separated peaks.

High performance liquid chromatography (HPLC) and ultra-performance liquid chromatography (UPLC) refers to LC systems exploiting high pressure pumps, able to tolerate the back pressure resulting from utilizing small particles in the chromatographic columns. Typical HPLC column particles lie in the range of 2.7-3.5 µm, while an UPLC column can have particles as small as 1.6 µm (Waters, 2023).

2.2.1 Columns

The stationary phase in LC is a solid or liquid material that is chemically bonded or coated onto a support material, usually silica, packed into a column. The choice of stationary phase depends on the separation requirements and the nature of the analytes.

2.2.1.1 Normal-phase chromatography

Normal-phase (NP) chromatography utilizes a polar stationary phase, such as silica, amino, or cyano groups, and a nonpolar mobile phase. NP chromatography is particularly effective for separating analytes that are soluble in nonpolar solvents and exhibit interactions with polar functional groups (Abbott, 1980). The separation mechanism is based on the differential affinity of analytes for the stationary phase, where interactions involve hydrogen-bonding and dipole-dipole interactions (**Figure 5a**). Nonpolar components have low affinity for the stationary phase and elute first, while polar analytes adsorb to the bonded functional groups and are retained longer.

2.2.1.2 Reversed phase chromatography

Reverse phase (RP) is the most widely used technique in LC (Skoog et al., 2018). The stationary phase consists of a non-polar material, such as C18, C8 or phenyl groups. RP columns are used for the separation of non-polar to moderately polar compounds based on

hydrophobic interactions (**Figure 5b**). The mobile phase is a polar solvent or mixture of solvents, such as water and organic modifiers. Polar analytes have weak interactions with the nonpolar stationary phase and elute first, while nonpolar analytes have stronger interactions and are retained longer on the column. By modifying the proportion of water and organic modifiers, the polarity of the mobile phase can be altered, influencing the partitioning behavior and separation of analytes.

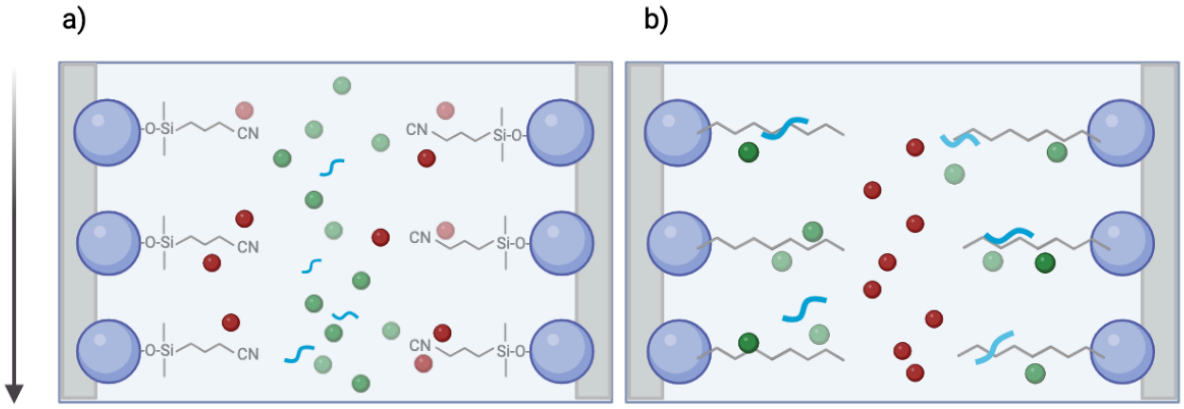

Figure 5. LC-separation mechanisms. a) Normal phase. Polar components (red) are retained through adsorption to the polar stationary phase. Nonpolar components (green and blue) have a higher affinity for the nonpolar mobile phase and are retained less. b) Reverse phase. Nonpolar components (green and blue) are retained through hydrophobic interactions. Polar components (red) are excluded.

2.2.1.3 Hydrophilic interaction liquid chromatography

Hydrophilic interaction liquid chromatography (HILIC) is a mode of chromatography that is specifically designed for the separation of polar compounds which are not adequately retained or separated using RP chromatography (Alpert, 1990). Separation is based on partitioning, electrostatic interactions, and hydrogen bonding with a hydrophilic stationary phase.

HILIC can be seen as a counterpart to NP chromatography, as both methods utilize a polar stationary phase, such as bare silica or a silica gel with polar functional groups. The main distinction between HILIC and traditional NP chromatography lies in the inclusion of water in the mobile phase, leading to differential retention mechanisms. In HILIC, the mobile phase consists of a water-miscible organic solvent, usually ACN, with the addition of a buffer and at least 2-3 % of water (McCalley, 2017). The water molecules concentrate at the surface of the polar stationary phase, creating a water enriched layer. Retention occurs as the analytes partition between the mobile phase and the partially immobilized water-enriched layer adsorbed onto the stationary phase (**Figure 6a**). More hydrophilic components are retained

withing the water layer longer compared to less hydrophilic components. The degree of retention increases with a higher concentration of organic solvent in the mobile phase and decreases with a higher concentration of water in the mobile phase.

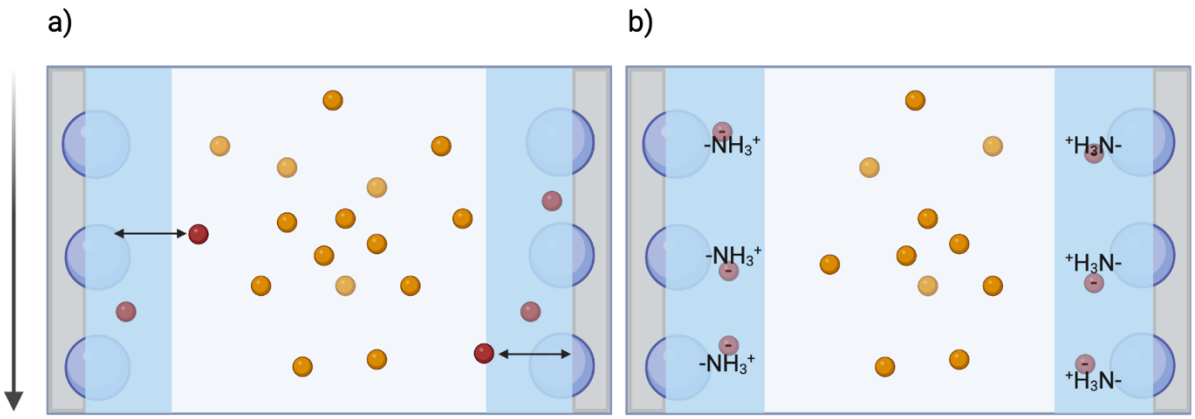

Figure 6. HILIC separation mechanisms. a) partitioning of polar component into a stationary water layer and b) electrostatic interactions.

A secondary separation mechanism is electrostatic interactions (**Figure 6b**), which occurs between charged stationary phase sites and charged analyte moieties (Greco & Letzel, 2013). The strength of electrostatic interactions depends on the extent of ionization of the analyte and ionizable groups on the stationary phase. This could be controlled by altering mobile phase pH and buffer strength in consideration of the analyte and column pK_a values. Furthermore, hydrogen bond formation between the stationary phase and the analyte increases retention of components with hydrogen bond donors.

2.2.2 Detection

Analytes eluting from the column can be detected by various techniques. Choice of detector is based on the nature of the analyte and potential interferences from matrix components. Furthermore, the detectors selectivity and sensitivity must be considered. Selectivity refers to the ability of a detector to recognize an analyte with a specific property, while leaving others undetected. Sensitivity refers to the increase in signal response with an increase in analyte concentration. The lowest detectable signal which is adequately separated from the baseline noise is the limit of detection (LOD) and is usually estimated to three times the height of the average baseline noise. Detection with high sensitivity is typically associated with low LOD and makes it possible to measure low levels of the analyte. Fluorescence spectroscopy and mass spectrometry are both selective and sensitive methods and will be discussed further.

2.2.2.1 Fluorescence spectroscopy

Fluorescence is when a substance absorbs light energy at a specific wavelength, and then re-emits light at a longer wavelength (Skoog et al., 2018). This occurs due to the electronic transitions within the molecule. When a fluorescent molecule is exposed to light of a specific wavelength, the excitation wavelength, electrons within the molecule absorb the energy from the photons in the light source. The absorbed energy causes the electrons to transition from their ground state to higher energy levels, the excited state. The electrons will rapidly return to its ground state, a process called relaxation. The excess energy absorbed during excitation is released as photons, which have lower energy compared to the absorbed photons. This emitted light is known as fluorescence. Molecules with delocalized π-electrons can allow for absorption and emission of light. Examples are aromatic hydrocarbons such as naphthalene, anthracene, and polycyclic aromatic hydrocarbons.

A fluorescence detector generally consists of four components: a light source (lamp), an excitation grating, an emission grating, and a photomultiplier (**Figure 7**). The chromatographic column is connected to the flow cell which receives light beams of a specific wavelength. The light emitted from the fluorescent compound in the flow cell is split by the emission grating. The photomultiplier detects, amplifies, and converts the photon energy to an electrical signal.

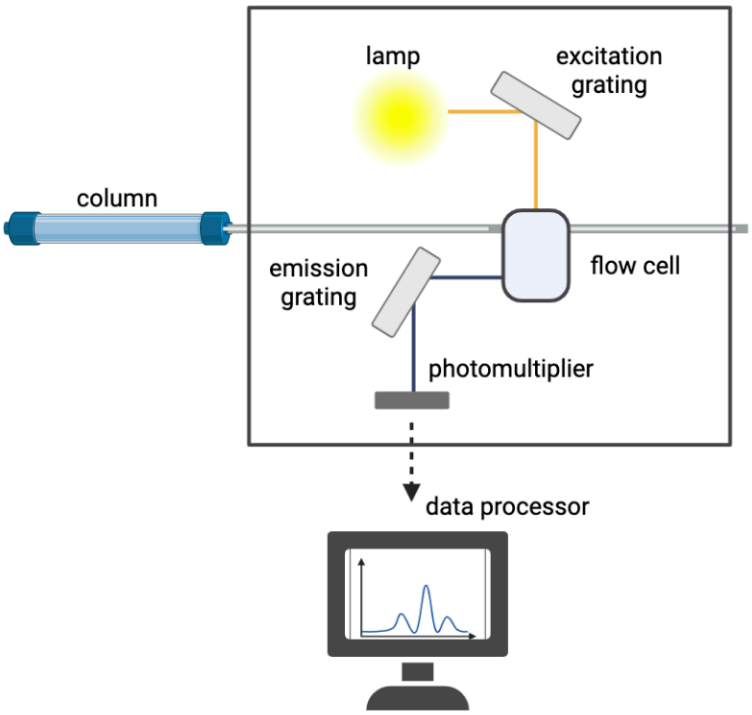

Figure 7. Fluorescence detector. Once analytes are eluted from the column, they enter a flow cell where they are exposed to light beams of a certain wavelength. The light source is a lamp, usually xenon, and the excitation grating separates the light to the specified wavelengths. The emitted light from the fluorescent analyte is split by the emission grating and converted to an electrical signal by the photomultiplier. The electrical signal is processed by a computer. Adapted from Shimadzu (2023a).

Fluorescence detection is highly sensitive, allowing up to 1000-fold increase in sensitivity compared to absorbance measurements (Bachmann & Miller, 2020). Another advantage of fluorescence compared to UV-vis absorbance is that fluorescent molecules are less abundant than UV-absorbing molecules, making them easier to detect within complex mixtures. Fluorescence detection is a selective method as it relies on the specific excitation and emission wavelengths of the analyte. In addition, the results are not affected by interference from the mobile phase, or other non-fluorescent components.

2.2.2.2 Mass spectrometry

Mass spectrometry (MS) is a detection method used to determine the molecular weight of charged molecules based on their mass-to-charge (*m/z*) ratio. The *m/z* ratio is the mass (m) of the ion divided by the charge (z). Ions in MS are often singly charged, so the *m/z* ratio is equivalent to the mass of the ion (Skoog et al., 2018). Resolution in MS is a measure of the MS instrument's ability to resolve individual ions with similar *m/z* ratios and is expressed as a ratio of the nominal mass of the first peak to the mass difference between two adjacent peaks.

The principle of MS involves ionizing the sample molecules, separating the ions based on their *m/z* ratio, and measuring their abundance.

During ionization the molecules are converted to charged particles. Different ionization techniques exist, with electrospray ionization (ESI) (**Figure 8**) being the most common method for coupling LC with MS (Santa, 2013). The sample solution is passed through a capillary tube with a high voltage. The strong electric field causes the solvent to be ionized, resulting in charged droplets (Shimadzu, 2023b). The repulsive forces between the charged droplets lead to fission into smaller droplets. As the charged droplets move through the heated region of the electrospray source, solvent molecules begin to evaporate from the droplets due to the high temperature. Continued solvent evaporation leads to reduction in droplet size until formation of gas-phase ions. These ions are then drawn into the mass spectrometer for further analysis.

ESI can be operated in either positive or negative mode, the difference being the generation and detection of positive or negative ions, respectively. The choice of ionization mode depends on the properties of the analyte. Analytes with basic characteristics are often analyzed in positive ion mode, where the analyte acquires a proton (H^+) from the solvent solution (Bruker, 2014). Acidic analytes are generally analyzed in the negative mode, with loss of a proton to a base in the solution. This leads to formation of molecular ions denoted $[M+H]^+$ or $[M-H]^-$.

$$M^0 + HA \leftrightarrows [M+H]^+ + A^-$$

$$M^0 + B \leftrightarrows [M-H]^- + HB^+$$

Polar neutral species that are not protonated or deprotonated in solution can also be ionized in the ESI ion source by adduct formation with Na^+, K^+ and NH_4^+ (positive mode), or with $CHOO^-$, CH_3COO^- and Cl^- (negative mode). Polar solvents such as water, methanol or acetonitrile (ACN) are generally used. The pH of the solvent influences the ionization efficiency, and volatile additives such as formic acid or ammonium hydroxide are used to adjust the pH. A desirable pH for positive ions is <7.0 and >7.0 for negative ions.

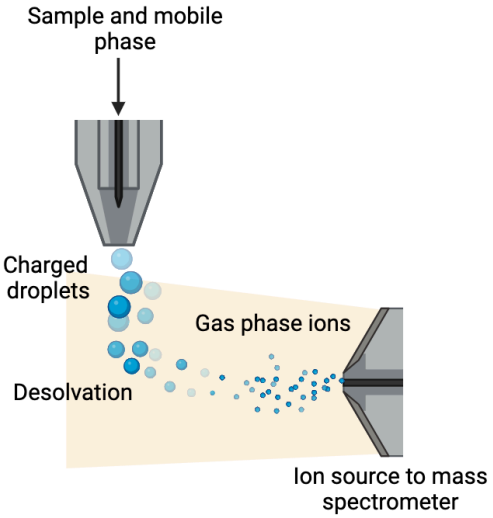

Figure 8. Simplified schematic of electrospray ionization. The sample is passed through a capillary tube containing a high voltage, which causes charged droplets to form. The solvent is evaporated due to the high temperature of the drying gas. Gas phase ions are introduced to the mass spectrometer. Adapted from Shimadzu (2023b).

The second step is ion separation, where the ions are subjected to a mass analyzer which separates them based on their *m/z* ratio. There are different mass analyzers, such as time-of-flight (TOF) and quadrupole. The TOF analyzer (**Figure 9a**) separates ions based on the time it takes for them to travel a known distance. The ions are accelerated into a flight tube by applying high voltage to give each ion a potential energy corresponding to its charge multiplied with the voltage. As the accelerated ions enter the flight tube, they travel a specific distance towards the detector. Two ions of the same charge but different masses will receive the same energy but will travel at different velocities, and thus reach the detector at different times. The flight time of the ions is measured, which is directly related to their *m/z* ratio. By comparing the flight times of different ions, their masses can be determined. TOF analyzers offers the highest resolution, fastest scan speed, and unlimited *m/z* range, compared to the quadrupole analyzer (Kaklamanos et al., 2016). The quadrupole mass analyzer (**Figure 9b**) is based on the principles of radio frequency and direct current electrical fields to selectively convey ions of specific *m/z* ratios (Skoog et al., 2018). The instrument consists of four parallel metal rods which serve as electrodes. The beam of ions enters the quadrupole in the space between the four rods. The voltages set onto the rods generates a combination of radio frequency and direct current electric fields. These applied voltages on the rods can be adjusted to allow only ions within a specific *m/z* range to reach the detector by stable oscillations in the ion beam. All other ions will have unstable oscillations and are ejected away from the linear

ion beam trajectory. By varying the voltages applied to the rods, different *m/z* ranges can be scanned, allowing for acquisition of full mass spectra.

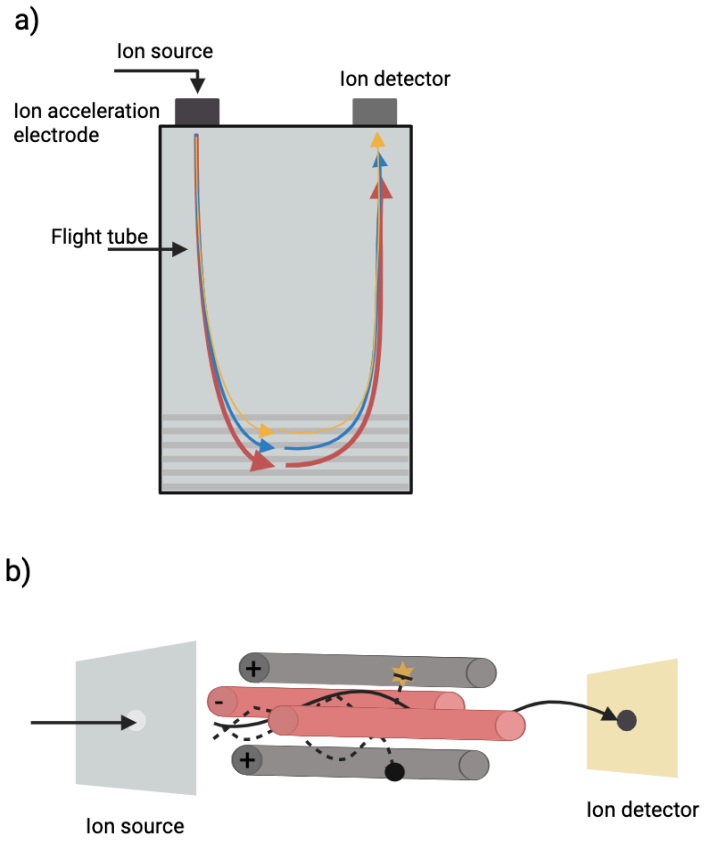

Figure 9. Simplified schematics of mass analyzers. a) Time of flight mass analyzer. Ions are accelerated by application of an electric field, causing the ions to accelerate. The ions enter the flight tube where they travel at constant velocities based on their *m/z* ratio. Lighter ions will move faster than heavier ones. The detector measures the arrival time of the ions. b) Quadrupole mass analyzer. Ions with *m/z* ratios that correspond to the stable trajectories (regions of stability within the quadrupole) can pass through the quadrupole and exit, while ions with other *m/z* ratios are repelled and collide with the rods. Figures adapted from Shimadzu (2023c).

The separated ions are then identified by a detector, which records the abundance of ions at specific *m/z* ratios. Common detectors are electron multipliers or ion-to-photon detectors consisting of a scintillation device coupled with a photomultiplier tube. The detected ions are converted into mass spectra, which represents the abundance of ions at different *m/z* values. The resulting data can be analyzed by e.g., database searching or fragmentation pattern analysis. The fragmentation pattern is specific to the molecular structure of the analyte.

Tandem mass spectrometry (MS/MS) uses two or more connected mass analyzers and is useful for increasing the selectivity of the MS detection. It can be applied for detection of

small molecules and is also useful for elucidating the structure of large biomolecules such as proteins and peptides (Hunt et al., 1986). The analytes are ionized before reaching the first mass analyzer which separates the ions based on their *m/z* values. Ions of a particular m/z ratio are selected into a collision cell where they are split into smaller fragment ions. These fragment ions are then introduced into the second mass analyzer, where they are further separated based on their *m/z* values. The resulting MS/MS data can be used to characterize and identify analytes based on specific fragmentation patterns.

2.3 Sample preparation

Sample preparation in analytical chemistry refers to the process of transforming a raw sample into a form suitable for analysis. It aims to extract the analytes of interest while removing interfering substances that may affect the accuracy and sensitivity of the analytical method. In addition, the sample must be compatible with the analytical technique. Common procedures involved are centrifugation, extraction, filtration, enrichment or dilution, and derivatization. Sample preparation regarding blood samples will be discussed further.

2.3.1 Sample collection and storage

Proper sampling technique is crucial to minimize the risk of contamination of the sample, infection, or injury to the patient. Blood sampling is therefore performed by a trained biomedical laboratory scientist. Blood is drawn into collection tubes, which can be coated with an anticoagulant such as ethylenediaminetetraacetic acid (EDTA) (Banfi et al., 2007). EDTA prevents coagulation by forming a complex with calcium ions, which inhibits formation of fibrin clots. If the tube does not contain an anticoagulant, blood clotting occurs, and blood cells and some proteins precipitate. Centrifugation of the sample separates the particles from the liquid plasma or serum (**Figure 10**). Since no anticoagulants are used in serum, fibrinogen and associated proteins are removed through the clotting process (Pawula et al., 2013). The advantage with using plasma is that blood can be centrifuged instantly after collection, which reduces the risk for hemolysis. After centrifugation, the supernatant can then be collected carefully and transferred to new tubes for storage or further processing. If the samples are not analyzed immediately, they should be stored in a freezer at -20 ˚C or -80 ˚C.

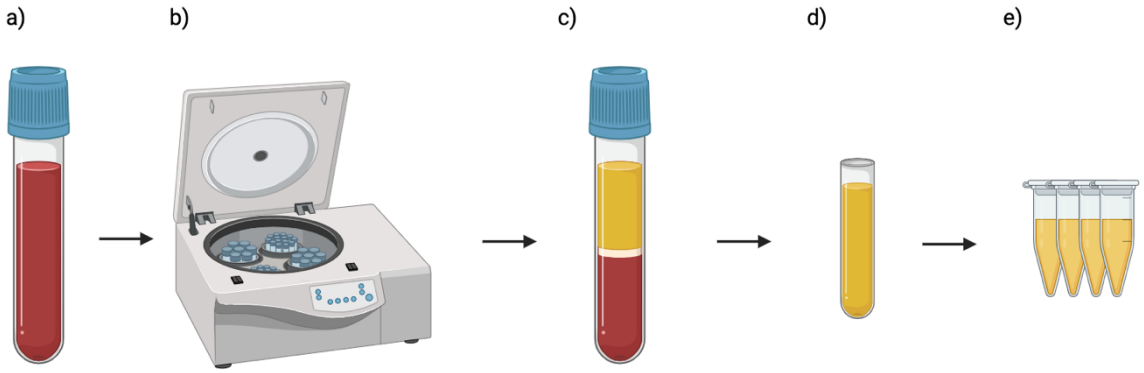

Figure 10. Blood sample collection. a) blood sample collected from patient b) centrifuge c) after centrifugation, the top layer (plasma or serum) can be carefully collected and transferred to a new tube. e) The plasma or serum is pooled and mixed. e) the plasma or serum is aliquoted into smaller tubes for storage.

2.3.2 Extraction

Extraction methods aims to separate the analyte from the sample matrix. Blood is comprised of different cell types, salts, gases, and large biomolecules such as carbohydrates, proteins, and lipids (Krebs, 1950). All these components are dissolvent in water, which makes up ~50 % of total blood volume. Several extraction methods exist, such as liquid-liquid extraction (LLE) and solid-phase extraction (SPE). Choice of extraction method will depend on the nature of the analyte and sample matrix. In LLE the components are partitioned between two immiscible solvents, e.g., an organic solvent such as diethyl ether and water (Lundanes et al., 2013). Nonpolar analytes are extracted into the organic phase, which can be collected and concentrated with evaporation of the solvent. In SPE, the liquid sample is passed through solid phase of sorbent particles, packed into a cartridge (Poole, 2003). The analytes are trapped on the surface of the solid phase, while matrix components pass through. A suitable sorbent is chosen based on the properties of the analyte and sample solvent. Different sorbents are available, including RP, NP, and ion-exchange. The analyte is eluted using an appropriate elution solution, after matrix components are washed out from the cartridge. SPE offers several advantages over traditional LLE, such as faster processing times, reduced solvent consumption, and analyte enrichment. In addition, on-line SPE coupled to LC-MS/MS instruments reduces sample preparation time and can achieve low limits of detection (LODs) (Naldi et al., 2016).

2.3.3 Protein precipitation

Protein precipitation (PPT) is the removal of proteins from a liquid sample. It involves the addition of a precipitating agent to the solution, such as organic solvents and/or salts, causing denaturation of the proteins and subsequent aggregation (**Figure 11**). The protein precipitate can be separated from the supernatant using centrifugation or filtration. A 10 % (w/v) solution of trichloracetid acid is an especially efficient precipitating reagent which can remove 99.7 % of proteins with a reagent solution-to-plasma ratio of only 0.2 (Blanchard, 1981). Organic solvents such as ACN, acetone, ethanol, and methanol will also remove proteins affectively, but requires a larger solvent-to-plasma ratio. Choice of reagent or solvent usually depends on compatibility with the analysis method.

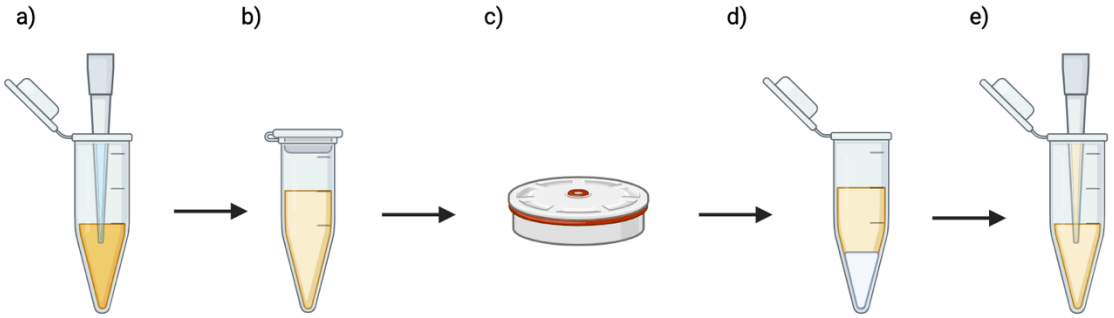

Figure 11. Protein precipitation. a) A PPT solvent is added to plasma or serum before b) mixing the liquids. c) the sample is centrifuged which d) separates the proteins (bottom) from the supernatant (upper layer). The supernatant can be carefully collected with a pipette and e) transferred to a new vial.

2.3.3 Derivatization

Derivatization is the process of altering physical and/or chemical characteristics of an analyte molecule (Cardinael et al., 2015). In LC, this process is commonly employed for analytes that have either no or low detectability. In addition, it is possible to enhance the retention of polar analytes in RP-LC by introducing hydrophobic groups and/or removing polar groups. Derivatization can be accomplished through chemical reactions between the analyte and a derivatization reagent. The signal from the derivatization reagent should be distinguishable from that of the analyte, or ideally, undetectable altogether.

Fluorescence detection is a particularly sensitive detection method, enabling detection of minute concentration of analytes. A study by Yoshitake et al. (2005) reports detection limits down to 4.0 fmol/mL by derivatizing neurotransmitters with benzylamine. Derivatization of amino acids into fluorescing compounds have been reported in several studies using reagents

such as phtpalaldehyde (Lindroth & Mopper, 1979), 9-fluorenylmethyl chloroformate (Bank et al., 1996), and dansyl chloride (Takeuchi, 2005).

Molecules with low ionization efficiency in MS analysis often requires large volumes of sample to a achieve satisfactory signal output. Derivatization can solve this problem by attachment of a readily ionizable or permanently charged group. One example is the butanolic hydrochloric acid (HCl) derivatization of carboxylic acids, which generates the more hydrophobic and ionizable butyl ester derivative (Santa, 2013).

2.4 Derivatization of G3P

G3P is not retained on RP columns and cannot be detected using UV-vis or fluorescence spectroscopy, due to its chemical and physical properties. However, derivatization using suitable reagents offers a potential solution to achieve both retention and detection of G3P. Addition of hydrophobic groups to either the hydroxyl- or phosphate groups could enhance retention on RP columns. In addition, if the derivatization reagent contains a chromophore or fluorophore, the analyte could be detected with UV-Vis or fluorescence spectroscopy. If sufficient reaction yield, small amounts of G3P could be analyzed in plasma samples. G3P contains two acidic groups which are possible to react with alcohols in an esterification reaction (**Figure 12**).

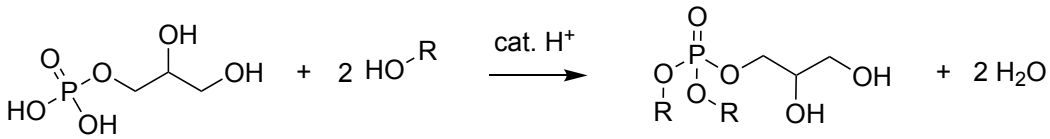

Figure 12. Possible esterification reaction of G3P with an alcohol.

Esterification reactions are generally described for carboxylic acids, acid anhydrides and acid chlorides (Khan et al., 2021). Synthesis of phosphoester bonds have been described, often using coupling agents such as aryl sulfonyl chlorides, imidazoles, triazoles or tetrazoles (Keana et al., 1986; Williams & Boehm, 1995). Esterification of phosphoric acid with alcohols using activating species such as acetic anhydride gives monoesters (Dueymes et al., 2008). In living cells, phosphate transfer reactions are prevalent. For instance, G3P is formed from glycerol and ATP catalyzed by glycerol kinase. Phosphate transfer reactions are generally catalyzed by enzymes containing magnesium ions, which makes the phosphorus atom more electrophilic by increasing the dipole moment of the phosphorus oxygen bond

(Soderberg, 2019). One of the proposed mechanisms for phosphoryl transfer reactions is an S_N2-like reaction, where the nucleophile approaches the electrophilic center opposite from the leaving group. The leaving group in a glycerol kinase catalyzed phosphorus transfer reaction is adenosine diphosphate. An alternative mechanism is the addition-elimination reaction, where the leaving group is expelled after the nucleophile binds to phosphorus. Neither the S_N2-like or the addition-elimination mechanisms would give the desired product from **Figure 12**, as glycerol would be the preferred leaving group. A proposed mechanism for the acid catalyzed esterification reaction of G3P is presented in **scheme 1**. The mechanism is like a Fischer esterification reaction for carboxylic acids. The nucleophilic oxygen of the alcohol attacks the electrophilic phosphate at the phosphorous center. The catalytic proton facilitates the nucleophilic attack by making the phosphorus atom more electrophilic. Proton transfer from the nucleophile to one of the hydroxyl groups creates H_2O, a good leaving group. The water molecule is expelled as the double bond between phosphorus and oxygen is regained. The last step is regeneration of the catalyst.

Esterification reactions are generally slow and reversible. There must be a continuous removal of water and/or addition of an excess amount of one reactant, usually the alcohol (Khan et al., 2021). The reaction yield is limited due to establishment of a thermodynamic equilibrium. A low reaction yield is not necessarily a problem for analytical purposes, as the most important factor is reproducibility.

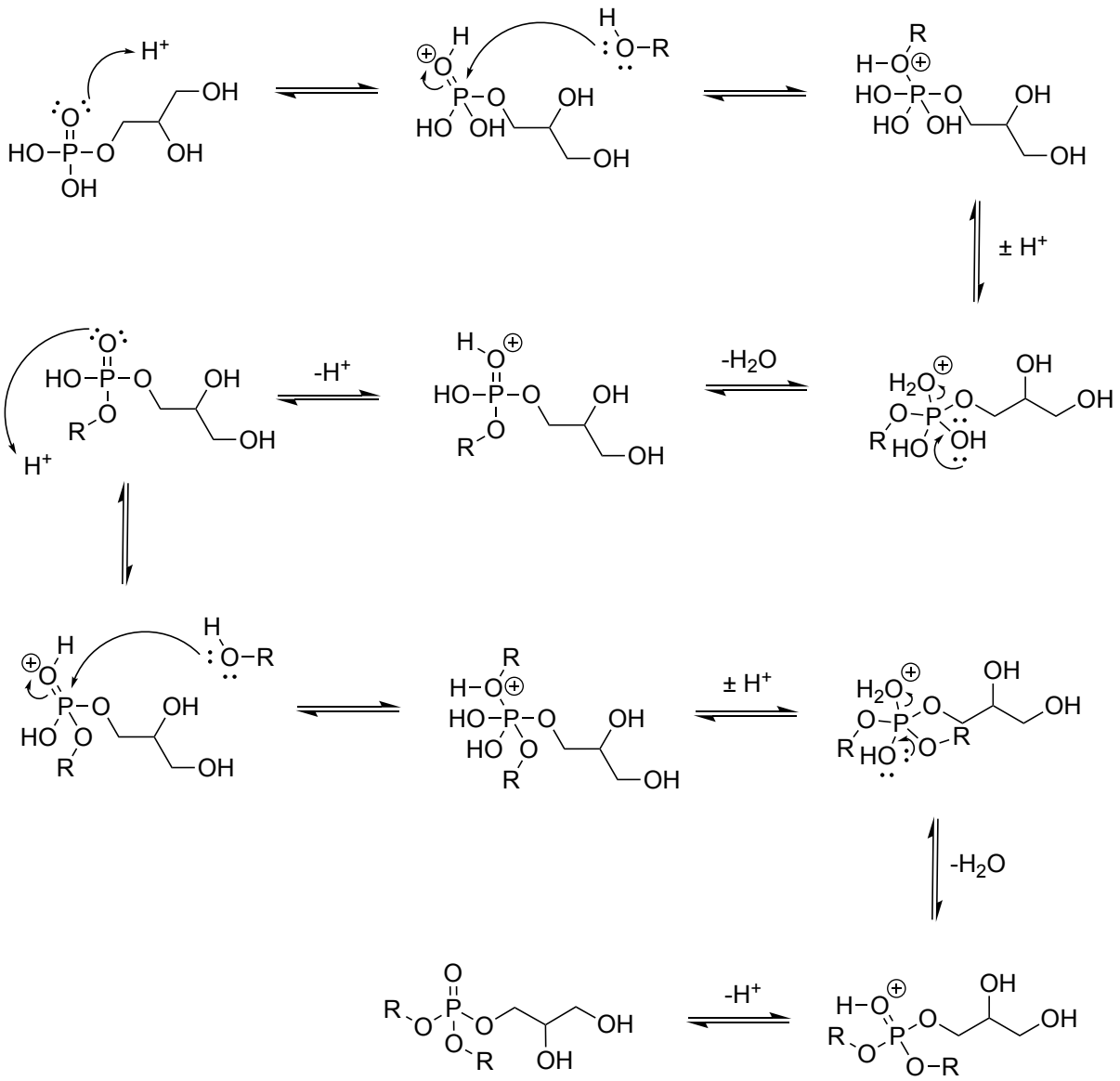

Scheme 1. Proposed mechanism for esterification of G3P.

3 Experimental

3.1 Chemicals and equipment

3.1.1 Chemicals

Organic solvents. Acetonitrile (≥99.9 %), acetone (≥99.9 %), butan-1-ol (99.6 %) and propan-1-ol (≥99.8) from VWR International (Radnor, Pennsylvania, USA). Methanol (≥99.9 %) from Honeywell (Charlotte, North Carolina, USA). Ethanol (96 %) from Kemetyl (Vestby, Norge).

Acids. Hydrochloric acid (37 %) and formic acid (99 %) from VWR International. p-Toluenesulfonic acid monohydrate (97 %) from Thermo Fisher (Waltham, Massahusetts, USA). Phosphoric acid (85 %) from Sigma-Aldrich (St. Louis, Missouri, USA).

Buffers and salts. Phosphate buffered saline (PBS) tablets from Amresco (Solon, Ohio, USA). Ammonium acetate (98 %) from Honeywell. Ammonia solution (25 %) from Suprapur Supelco (Darmstadt, Germany). sn-Glycerol 3-phosphate bis(cyclohexylammonium) salt (93 %) from Sigma-Aldrich. ^{13}C3 Glycerol-3-phosphate (sn-[UL-$^{13}C_3$]glycerol 3-phosphate disodium salt) (99 %) from Omicron Biochemicals Inc. (South Bend, Indiana, USA).

Fluorescent derivatization reagents. 1-Napthalenemethanol (98 %), 9-Fluorenemethanol (99 %), and 9-Anthracenemethanol (97 %) from Sigma-Aldrich.

Sample material. Autonorm™ immunoassay from SERO AS (Bilingstad, Norway).

3.1.2 Equipment

Tubes and vials. 4.0 mL glass vials with teflon lined caps used for derivatization of G3P with 9FlMe from Teknolab (Kolbotn, Norway). 0.3 mL PP Short Thread Micro-Vial 32 x 11.6 mm, transparent, with screw caps used for HPLC-F and LC-MS analysis from VWR. Nunc U96 Microwell Plate 0.5 mL, equipped with a Nunc 96-well cap mat. Non-sterile., and 30 mL glass bottles from Thermo Fisher. 9 mL EDTA tubes from VWR and 1.5 mL micro tubes from Sarstedt (Nümbrecht, Germany), were used for blood sampling and processing.

Centrifuges. For micro tubes: Tabletop Micro Refrigerated Centrifuge from Kubota, (Tokyo, Japan). For well-plates: Heraeus Multifuge 3 S-R from Thermo Fisher. For blood sample tubes: Universal 320 R from Hettich (Tuttlingen, Germany). Vacuum centrifuge for evaporation of water: Genevac, miVac Duo concentrator from Thermo Fisher.

Spectrophotometer. A UV-1700 PharmaSpec UV-Vis spectrophotometer was used for measurements of absorption wavelength from fluorescent compounds, from Shimadzu (Kyoto, Japan).

HPLC-F. HPLC separation of derivatization products from G3P 9FlMe was carried out on a prominence LC-20AD liquid chromatograph coupled to a RF-20A fluorescence detector, both from Shimadzu. The column used was a SunShell C18 column (2.1 mm x 150 mm, 2.6 µm particle size) from ChromaNik Technologies (Osaka, Japan). Software used for data analyzation was Labsolutions from Shimadzu.

LC-MS. An Acquity UPLC I-class LC from Waters (Milford, Massachusetts, USA) coupled to a timsTOF mass spectrometer from Bruker (Billerica, Massachusetts, USA) was used for analysis of fractions from HPLC separation of G3P 9FLMe derivatization products. The chromatographic column was an Acquity UPLC BEH c18 (2.1 mm x 50 mm, 1.7 µm particle size) from Waters. The software used to control the LC and MS was Compass HyStar and otofControl from Bruker.

LC-MS/MS. Analysis of G3P butyl diesters was performed on an Acquity UPLC liquid chromatograph coupled to a Xevo TQ-S Triple Quadrupole Mass Spectrometer, both from Waters. The chromatographic column was an Acquity UPLC BEH C18 (2.1 mm x 50 mm, 1.7 µm particle size) from Waters. The software MassLynx from Waters was used to analyze the LC-MS output.

HILIC-MS. Analysis of G3P was performed on an Acquity UPLC I-class from Waters coupled to a timsTOF mass spectrometer from Bruker. The chromatographic column was an Acquity UPLC BEH Amide (1.7 µm, 2.1 x 100 mm) column from Waters. The software used to control the LC-MS system was Compass HyStar from Bruker.

3.2 Derivatization procedures

3.2.1 Preliminary evaluation of fluorescent derivatization reagents

Stock solution of 9AnMe, 1AnMe and 9FlMe were prepared by weighing 5.0 mg of each compound in 30 mL glass vials before dissolving the solid in 20 mL ACN. User solutions of 150 ng/mL were prepared by diluting the stock solutions with ACN. The solutions were analyzed with a spectrophotometer to find optimal absorption wavelengths. Excitation and emission wavelengths reported for similar compounds (anthracene,

naphthalene, and fluorene) by Joseph (n.d) and Jing et al. (n.d) were used in HPLC-F analysis (**Table 1**). The mobile phase was A: 0.05 % phosphoric acid in water and B: 0.05 % phosphoric acid in ACN. Elution was gradient (**Table 2**) with a 12 min total run time.

Table 1. Excitation and emission wavelengths used in preliminary testing of derivatization reagents.

Compound	Ex/Em wavelengths (nm)	Reference
Anthracene	247/310	Jing et al. (n.d)
	252/402	Joseph (n.d)
Fluorene	263/310	Jing et al. (n.d)
	224/320	Joseph (n.d)
Naphtalene	219/330	Jing et al. (n.d)
	224/330	Joseph (n.d)

Table 2. Elution profile for 9AnMe, 1AnMe and 9FlMe. A is 0.05 % phosphoric acid in water and B is 0.05 % phosphoric acid in ACN.

Time (min)	A %	B %
Initial	80	20
1	80	20
2	50	50
5	10	90
9	80	20
12	80	20

Optimal excitation and emission wavelengths for 9FlMe were found by keeping one value constant (constant emission at 263 nm and excitation at 310 nm) and changing the other in intervals of 1, starting from excitation/emission 259/308 and ending at 275/325. Best signals, registered as peak heights, were recorded at excitation/emission wavelengths 265/310 nm for 9FlMe. These values were then used when analyzing G3P 9FlMe derivatization products.

3.2.2 Derivatization with 9-fluorenemethanol

Derivatization was achieved by weighing 0.60 mg (1.5 µmoles) of G3P in 4.0 mL glass vials. Then 29 µL of a 10 % (w/v) solution of 9FlMe in ACN (3.0 µmoles) was added to the

vial together with 5.6 µL of a 10 % (w/v) solution of the catalyst PTSA in ACN. The reaction solvent ACN was added to get a total volume of 4.0 mL. The vial was then placed in a drying oven at 110 °C for 1 h. The solvent evaporated during heating, so 4.0 mL of ACN was added before diluting to a theoretical concentration (if 100 % yield) to 2 000 ng/mL. Different conditions were tested by varying the mol ratios of G3P to 9FlMe (G3P:9FlMe 1:2-1:10) and % PTSA (5 % - 200 % (w/v) in ACN).

Analysis of derivatization reagents and derivatives was performed with HPLC-F using a C18 column. The column was eluted at a flow rate of 0.2 mL/min with initial conditions of 80 % mobile phase A, and 20 % mobile phase B with elution time of 23 min (**Table 3**). Mobile phase A: 0.05 % phosphoric acid in water and B: 0.05 % phosphoric acid in ACN. Injection volume was 3.0 µL.

Table 3. Elution profile for HPLC-F analysis of G3P 9FlMe derivatization products. A is 0.05 % phosphoric acid in water and B is 0.05 % phosphoric acid in ACN.

Time (min)	A %	B %
Initial	80	20
1	40	60
12	40	60
14	20	80
19	20	80
20	80	20
23	80	20

Analysis of derivatization products and fractions from HPLC separation was carried out using RP-LC-MS. MS analyses were obtained using ESI in the positive mode using full scan analysis with a mass range from 20 to 1000 *m/z*. Column temperature was 45 °C and mobile phase flow rate 0.2 mL/min. Mobile phase was A: 0.5 % formic acid in water and B: methanol. Elution was gradient with initial mobile phase composition of 99 % A and 1 % B (**Table 4**). Injection volume was 5.0 µL.

Table 4. Elution profile for LC-MS analysis of G3P 9FlMe derivatization products. A is 0.2 % formic acid in water and B is ACN.

Time (min)	% A	% B
Initial	99	1
0.5	99	1
2.0	10	90
3.0	10	90
3.1	99	1
5.0	99	1

MS analyses were obtained using ESI in the negative mode using full scan analysis with a mass range from 20 to 1 000 *m/z*. Capillary voltage was 4 200 V. Nitrogen gas was operated at 8.0 L/min and nebulizer at 2.0 bar.

3.2.3 Derivatization with butanol

50 µL sample and 200 µL solvent, MeOH, EtOH, PrOH or ACN were added to each vial of a microwell plate. The samples were Autonorm™ immunoassay serum, 200 µM G3P in PBS and blanks (PBS). There was a total of 4 replicates of each sample type and solvent. The plate was centrifuged (11min, 4 ˚C, 4000 G) before 50 µL of the supernatants were transferred to a new microwell plate. 20 µL of a 3.2 µg/mL internal standard solution ($^{13}C_3$ G3P) was added to each vial. The plate was then centrifuged under vacuum at 4000 G at 80 ˚C for 1 h until all solvent had evaporated. Then 200 µL 5 % (w/v) PTSA in BuOH was added to each vial. The plate was then placed on a hotplate for 1 h which held a temperature of 110 ˚C. 100 µL ACN and 100 µL water was added to each vial, and then the plate was shaken so that the solid products would dissolve. Then the plate was centrifuged (3 min, 4 °C, 4000 G) before transferring the supernatant to 0.3 mL micro-vials.

Analysis of G3P butyl diesters was performed using RP-LC-MS/MS. Mobile phase was A: 0.2 % formic acid in water and B: ACN. Elution was gradient with initial conditions of 99 % A and 1 % B with a total run time of 5.0 min (**Table 5**). Injection volume was 5.0 µL.

Table 5. Elution profile for LC-MS/MS analysis of G3P butyl diesters. A is 0.2 % formic acid in water and B is ACN.

Time (min)	% A	% B
Initial	99	1
0.5	95	5
1.0	90	10

1.5	43	57
4.0	37	63
4.1	5	95
4.2	5	95
4.21	99	1
5.0	99	1

The MS was operated in ESI positive mode. Multiple reaction monitoring (MRM) was used to selectively detect and quantify G3P butyl diesters. Three MRM transitions were set up for G3P- and $^{13}C_3$ G3P butyl diester molecular ions (**Table 6**). The response was calculated as the area from the peak from G3P butyl ester (*m/z* = 285.1) divided by the area from the G3P internal standard (*m/z* = 288.2).

Table 6. Molecular ($[M+H]^+$) and fragment (F^+) ions of G3P and 13C3 G3P butyl diester with capillary voltage, cone voltage and collision energy.

$[M+H]^+$ G3P butyl diester	F^+	Capillary (kV)	Cone (V)	Col. energy
285.1	99.1	3	20	18
285.1	173.1	3	20	11
285.1	229.2	3	20	8
$[M+H]^+$ $^{13}C_3$ G3P butyl diester				
288.2	99.1	3	20	18
288.2	176.1	3	20	11
288.2	232.2	3	20	8

3.3 Analysis of G3P using HILIC

G3P was analyzed directly using HILIC-MS. Elution was isocratic with a flow rate of 0.2 mL/min and a total analysis time of 6 minutes. Column temperature was 19 ˚C. MS analyses were obtained using ESI in the negative mode using full scan analysis with a mass range from 20 to 1 000 *m/z*. Capillary voltage was 4 200 V. Nitrogen gas was operated at 8.0 L/min and nebulizer at 2.0 bar.

3.3.1 Simplex optimization

A modified simplex was performed as described by Bezerra et al. (2016), for the optimization of mobile phase. The parameters chosen for optimization were ACN and salt concentration using isocratic elution. Peak height was used as the response factor. The initial variables were 20 % mobile phase A (water), 80 % mobile phase B (20/80 % water/ACN),

and 20 mM ammonium acetate and 20 mM ammonia in both A and B. The variation steps were 4 % and 3 mM for mobile phase B and salt concentration, respectively. Multiplication factors for calculating the vertexes for the initial simplex and α-values were retrieved from Bezerra et al. (2016). Two different samples were prepared. 0.50 mg G3P was dissolved in 3.0 mL MeOH or 5 % water in ACN. The solutions were then diluted to a concentration of 2.0 µg/mL. These samples were used for two parallel experiments to test how sample solvent influenced the response. Column equilibration time was estimated to take 35 min for each mobile phase change.

3.3.2 Variation of measured G3P between days

A 2 000 ng/mL G3P solution in MeOH was prepared and aliquoted into 15 0.3 mL micro-vials before analysis with HILIC-MS as described in section 3.2. Elution was isocratic with 19 % A (water) and 81 % B (20/80 % water/ACN) with 25 mM ammonium acetate and 25 mM ammonia in both A and B. The replicates were placed in the autosampler at 10 ˚C until analysis. Replicates 1-5 were analyzed on day 1, replicates 1-10 were analyzed on day 2, and replicates 1-15 were analyzed on day 6.

3.4 Sample preparation and G3P extraction

Blood samples were collected from two healthy individuals in 9 mL EDTA tubes and centrifuged (15 min, 2200 G, 4 ˚C). The plasma was then collected, mixed, and aliquoted into 1.5 mL micro tubes. The samples were stored at –20 ˚C before analysis. G3P was extracted from the plasma as described in Paynter et al. (2018). 30 µL plasma was added to a 1.5 mL micro tube together with 120 µL 80 % methanol. The sample was centrifuged (11 min, 4000 G, 4 °C) and the supernatant transferred to 0.3 mL micro-vials before analysis with HILIC-MS as described in section 3.3.2.

One experiment was set up testing different solvents for extraction of G3P and precipitation of proteins from plasma. 200 µL plasma was mixed with either 600 µL ethanol, 800 µL methanol, 400 µL acetone or 400 µL ACN in 1.5 mL centrifuge tubes and centrifuged (6 replicates of each solvent). Another experiment was set up where either EtOH or ACN was used for PPT. This time, the supernatant was evaporated at 60 ˚C before dissolving the remaining solids in 200 µL 1 % ammonium acetate in PrOH. Standard addition calibration was set up where 70 µL plasma was spiked with different concentrations of G3P, from 0 to 13657 ng/mL (**Table 7**). Water was added to get a total volume of 100 µL. The samples were

treated with 200 µL ACN for PPT, and the supernatant was evaporated at 60 ˚C before resuspending with 50 µL 1 % ammonium acetate in PrOH. This standard addition calibration was done twice. The extracts from these experiments were transferred to 0.3 mL micro vials and analyzed with HILIC-MS as described in section 3.3.2.

Table 7. Set up for standard addition calibration. G3P solution was 45524 ng/mL.

	Sample			
	1	2	3	4
Plasma (µL)	70	70	70	70
G3P solution (µL)	0	10	20	30
Water (µL)	30	20	10	0
G3P (ng/mL)	0	4 552	9 105	1 3657

3.5 The effect of heat and acid on G3P amount in plasma

24 samples were prepared, 12 were ACN was used for PPT and 12 were EtOH was used. 200 µL plasma was added to 1.5 mL micro tubes together with either 400 µL ACN or 600 µL EtOH. The tubes were centrifuged (11 min, 4000 G, 4 °C) before 100 µL supernatant from each tube was transferred to new tubes. The samples were set up as followed: 1,2,3: only supernatant. The samples were left in room temperature for 1 h. 4,5,6: only supernatant. The samples were heated at 110 ˚C for 1 h in a drying oven. 7,8,9: supernatant and 2 µL 5 % hydrochloric acid (HCl) in either ACN or etOH. The samples were left in room temperature for 1 h. 10,11 & 12: supernatant and 2 µL 5 % HCl in either ACN or EtOH. The samples were heated at 110 ˚C for 1 h in a drying oven. The solvent evaporated from the samples exposed to heat, so here 100 µL of solvent (ACN or EtOH) was added. The samples were centrifuged before the supernatant was extracted and transferred to 0.3 mL micro-vials. The samples were analyzed using the HILIC-MS set-up as described in section 3.3. Elution was isocratic with 16 % A (water) and 84 % B (20/80 % water/ACN) with 25 mM ammonium acetate and 25 mM ammonia in both A and B. Total run time was 6 minutes and injection volume 10 µL.

4 Results

4.1 Derivatization of G3P

Derivatization of G3P was carried out through an esterification reaction to gain retention with RP-HPLC. A fluorescent alcohol was applied for fluorescence detection while BuOH was utilized for MS detection.

4.1.1 Preliminary evaluation of fluorescent derivatization reagents

Three fluorescent compounds, 9-fluorenementhanol (9FlMe), 9-anthracenemethanol (9AnMe) and 1-naphtalenemethanol (1NaMe), were considered as reagents for derivatization with G3P for HPLC-F. Absorption wavelengths registered with the spectrophotometer were 264 nm for 9AnMe, 233 nm for 1NaMe and 275 nm for 9FlMe. All three compounds had satisfactory retention times and peak shapes with the method described in section 3.2.1. However, 9FlMe had six times higher peaks compared to 1NaMe and 9AnMe (see appendix I Figure I-23 for chromatograms). Derivatization was therefore proceeded with 9FlMe.

4.1.2 Derivatization with 9FlMe

Derivatization was attempted using heat (110 ˚C) and an acid catalyst (PTSA) as described in section 3.2.2. Two potential products were targeted (Figure 13); the mono- and diesters of G3P.

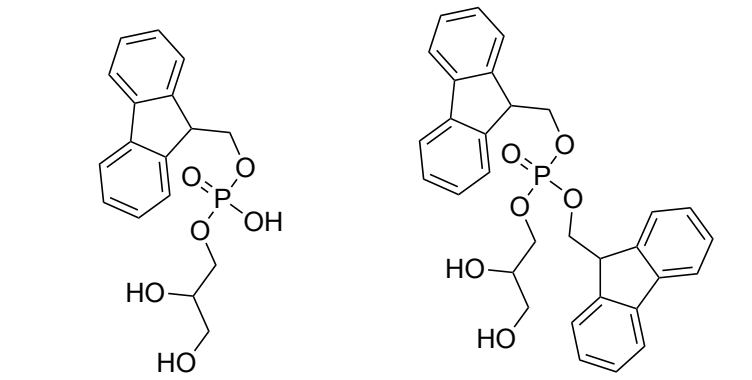

Chemical Formula: $C_{17}H_{19}O_6P$ Exact Mass: 350,09

Chemical Formula: $C_{31}H_{29}O_6P$ Exact Mass: 528,17

Figure 13. G3P 9FlMe mono- and diesters.

The products were analyzed with both HPLC-F. The chromatogram (**Figure 14**) of the reaction products revealed several new peaks. The highest peak (at 8.021 min) in the chromatogram originates from the reagent 9FlMe.

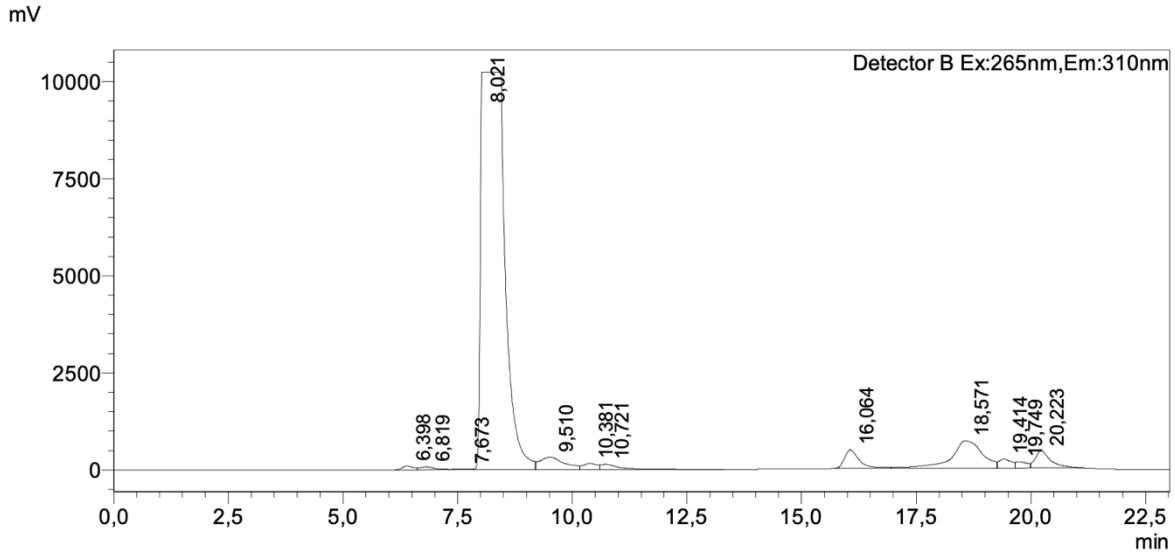

Figure 14. Chromatogram of products from G3P and 9FlMe derivatization. Peak at 8.021 min is the reagent 9FlMe.

Since no standards exist for G3P mono- and diesters of 9FlMe, HPLC-MS was utilized to scan for a molecular ion of the correct *m/z*. The mass spectrum revealed that G3P 9FlMe diesters were indeed formed, as a peak with *m/z* of 529.1784 was identified (**Figure 15a**). Fractions were collected from HPLC-F in minute intervals to identify which peaks belonged to the product. The diester product was identified in the interval 9-10 min, which corresponds to the peak at 9.510 min in **Figure 14**. However, the mass spectrum revealed that the diester product was only a minor contribution to the peak (**Figure 15b**).

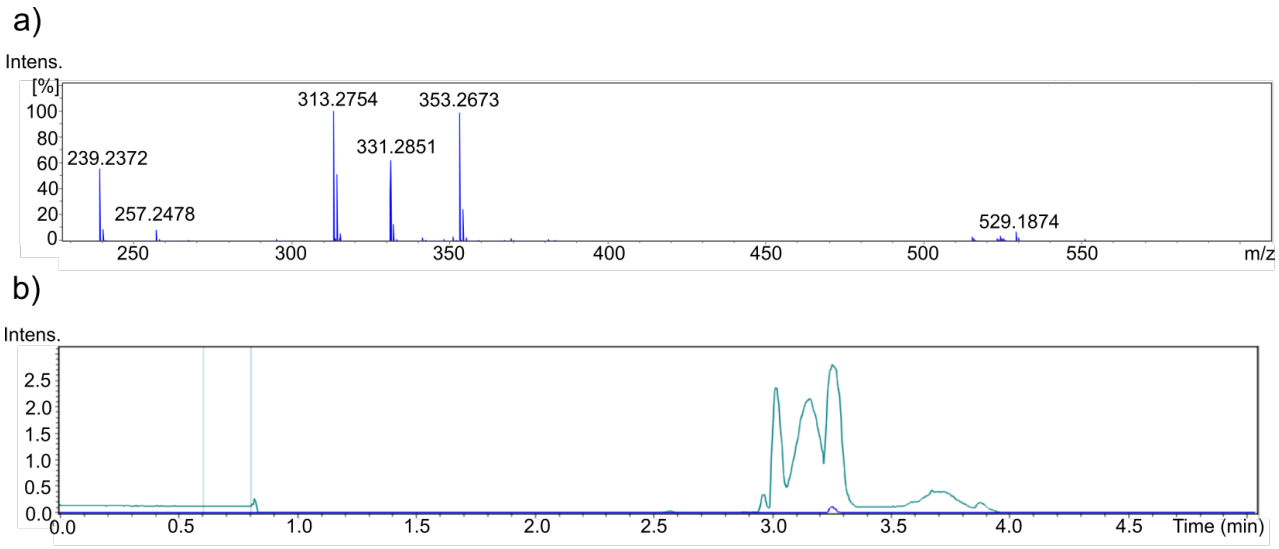

Figure 15. a) mass spectrum of fraction at 9-10 min retrieved from HPLC-F analysis. B) green: base peak chromatogram and blue: extracted ion chromatogram of m/z 529.17 ±0.005.

Several experiments using different concentrations of 9FlMe and PTSA were carried out to attempt to increase the peak height of the product. However, it was difficult to know if the increase in peak height was from an increase in product z concentration, or from an increase in biproducts. When the concentration of 9FlMe was increased, the peak width became larger, and it was difficult to separate the peak from the reagent with other small peaks in the chromatogram.

4.1.3 Derivatization with butanol

Butyl ester derivatization of methyl malonic acid in serum is a routine procedure at the department of medical biochemistry at SUS. Preliminary studies using the same protocol (not presented here) had revealed that G3P likely would derivatize with BuOH as well, resulting in diesters (**Figure 16**). However, there was a high degree of variability, with estimated concentrations of 53.7 and 119.5 µmol/L for two replicate control samples (see appendix II Table II-9 for analysis report).

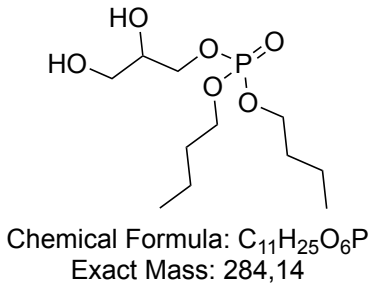

Figure 16. G3P butyl diester.

Serum, G3P in PBS and blank (PBS) samples were used in an experiment to test whether G3P could be derivatized directly after PPT. Different organic solvents, MeOH, EtOH, PrOH, and ACN, were used for PPT two test which would yield the most product. The results from LC-MS/MS analysis revealed that the diester product for G3P (*m/z* = 285.30) and G3P internal standard (*m/z* = 288.25) was present in all serum and G3P samples, with a retention time of 1.78 min (see appendix II Figure II-24 for chromatogram). The mean peak height was lowest for samples where ACN was used for PPT, while MeOH was particularly efficient in generating G3P butyl diesters (**Figure 17**).

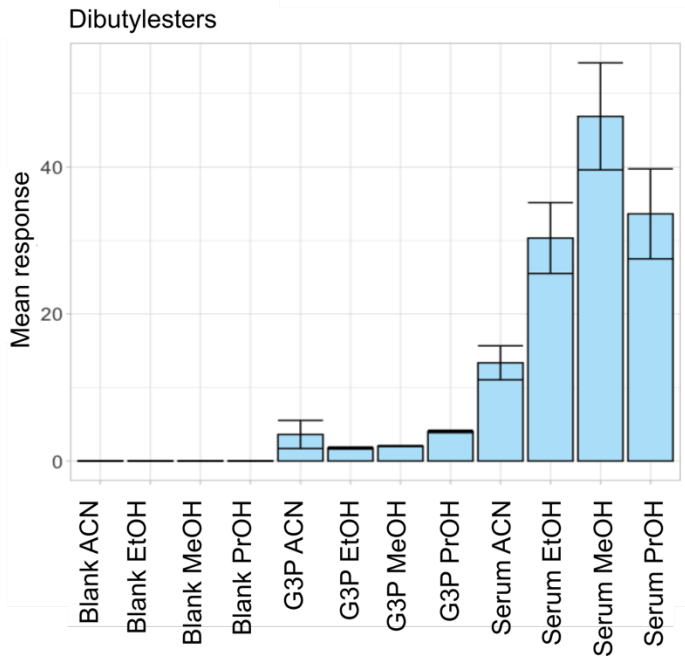

Figure 17. Bar plot of mean response with error bars from G3P butyl esters in serum, blank and in PBS.

4.2 Analysis of G3P using HILIC

G3P (*m/z* = 171.0058) was successfully retained and detected using HILIC-MS equipped with an amide column as described in section 3.3. Water, MeOH, water/ACN and PrOH with different salt concentrations were tested as sample solvents. Pure water was quickly excluded as an alternative since double peaking appeared in the chromatogram (**Figure 18a**). A solution of 40/40/20 % ACN/MeOH/water was tested as described in (Chiles et al., 2019), however peak splitting was observed here as well (**Figure 18b**). Addition of a small amount (5 %) in ACN or MeOH was possible without peak splitting.

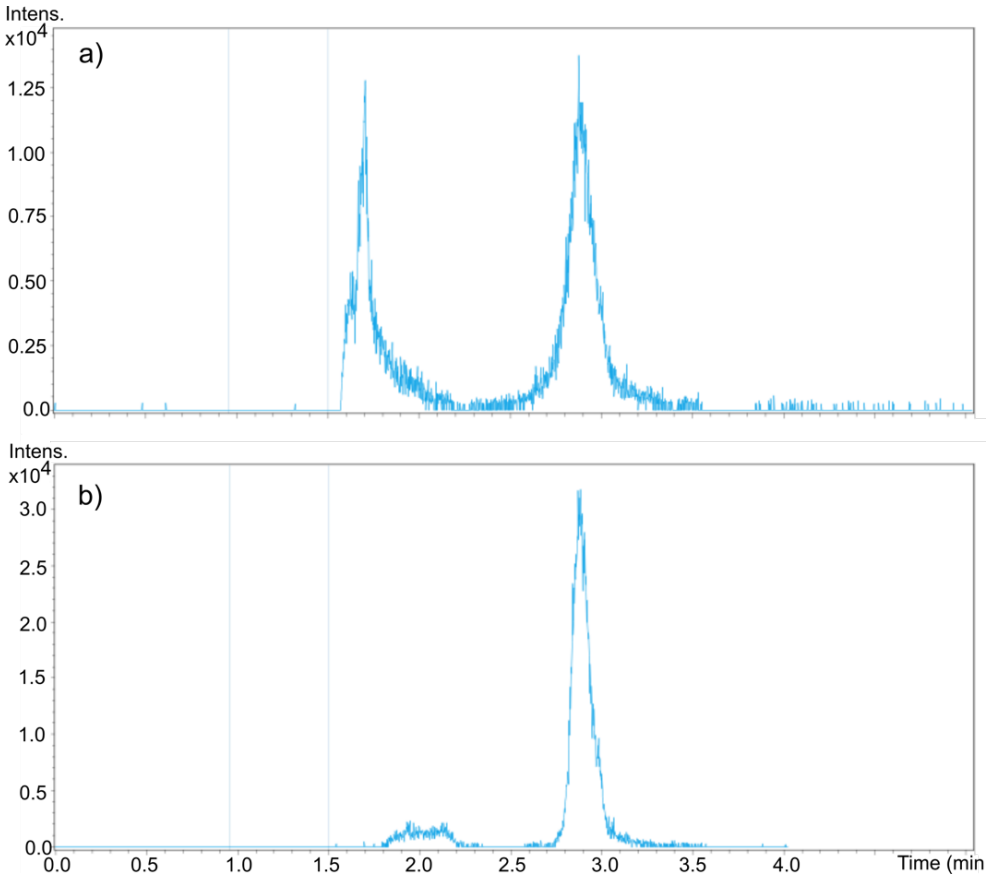

Figure 18. Double peaks observed on the extracted ion chromatogram of 1 240 ng/mL G3P in a) water and b) 40/40/20 ACN/MeOH/water analyzed with HILIC.

Different salt concentrations in the sample were tested. Increasing the amount of salt (ammonium acetate) from 1 % to 4 % in the sample (1 240 ng/mL G3P in PrOH) decreased the peak height (**Figure 19**) and lowering the salt concentration to 0.5 % decreased the peak height as well.

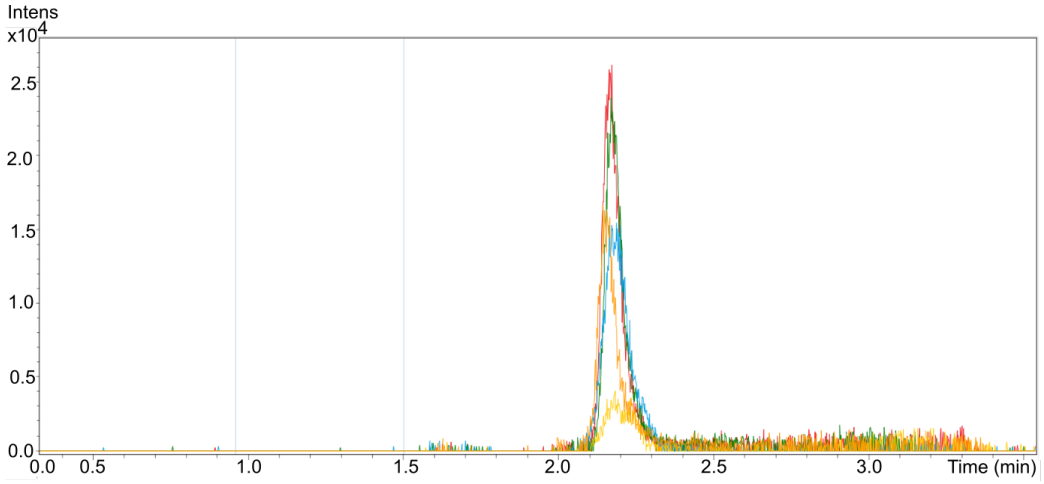

Figure 19. Extracted ion chromatogram (m/z = 171.0058±0.005) of G3P in PrOH with different salt concentrations (ammonium acetate %). Yellow: 4 %, blue: 3 %, orange: 0.5 %, green: 2 %, red: 1 %.

Changing the mobile phase composition from 56 % to 68 % ACN increased retention of G3P with just under 1 min (**Figure 20a**). Increasing the injection volume (G3P in 1 % ammonium acetate in PrOH) from 5 µL to 25 µL increased the retention time as well with just under 0.5 min (**Figure 20b**).

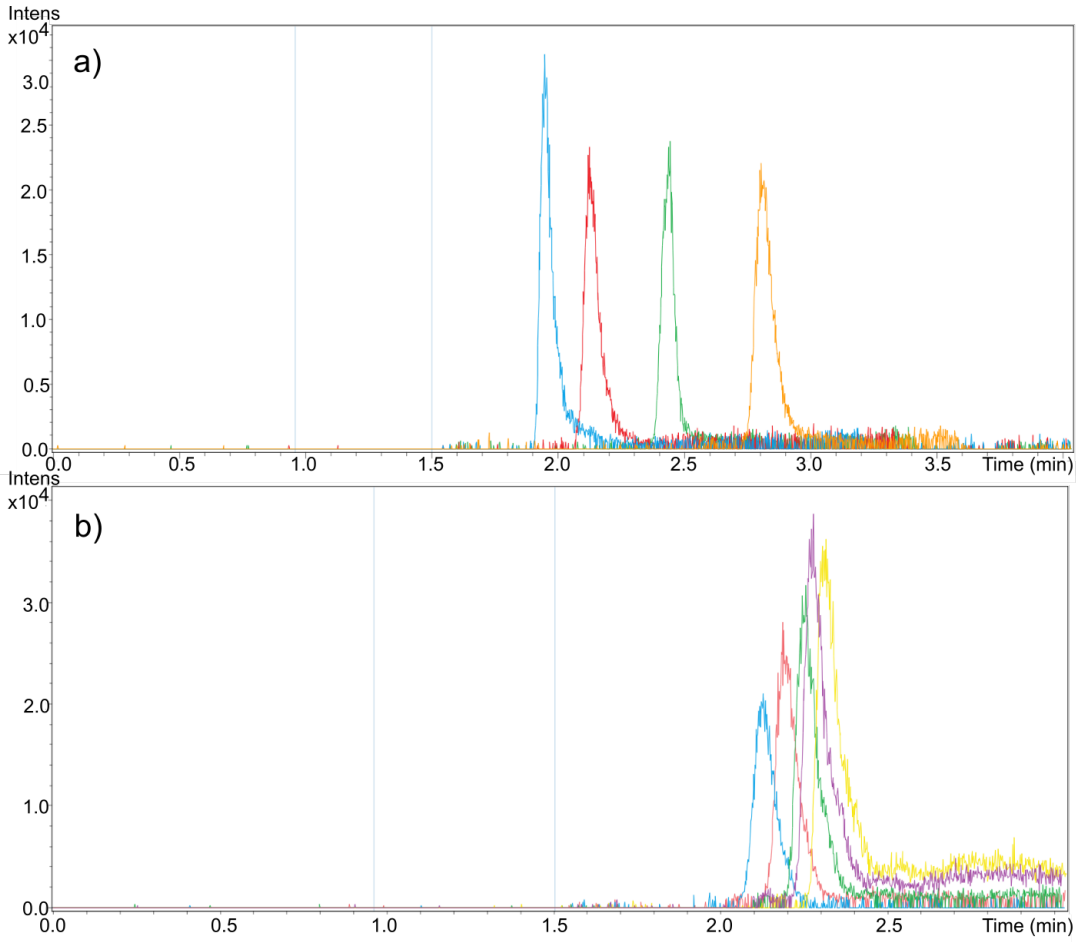

Figure 20. Extracted ion chromatograms (m/z = 171.0058±0.005) of G3P in PrOH with 1 % ammonium acetate. a) Increased retention of G3P with increased ACN % in the mobile phase Blue: 56 %, red: 60 %, green: 64 %, and orange: 68 %. b) increased retention of G3P with increased injection volume. Blue: 5 µL, red: 10 µL, green: 15 µL, purple: 20 µL, and yellow: 25 µL.

4.2.1 Simplex optimization

A modified simplex optimization was performed to try to find the ideal ACN and salt concentration in the mobile phase. The peak height was used as the response factor. The initial parameters were chosen based on preliminary testing and previous research (Chiles et al., 2019; Paynter et al., 2018). Initially, two parallel optimizations were performed, one with MeOH and one with 5 % water in ACN as sample solvents. Peak heights were notably higher for the G3P in MeOH sample. The experiments carried out are presented in **Table 8,** with results from the optimization using G3P in MeOH. The experiments were conducted over

several days, because of relatively long column equilibration time (35 min). During the experimentation, it was discovered that the response varied from one day to the next, using the same sample and mobile phase composition. Consequently, it was difficult to determine if the simplex was moving in the correct direction.

Table 8. Simplex optimization of ACN % and salt concentration (ammonium acetate and ammonia mM) in the mobile phase. Response is the peak height.

Experiment	Vertex	ACN %	Salt conc. (mM)	Response
1	I	64	20	30861
2	I	67.2	20	21321
3	I	65.6	22.6	33599
4	R	62.4	22.6	28775
5	CR	63.6	22.0	47063
6	R	65.2	24.6	48242
7	E	65.8	26.9	44333
8	R	63.2	23.9	47450
9	R	64.8	26.5	47259
10	CR	64.5	25.4	43033

4.2.2 Variation of measured G3P between days

15 replicates with 2 000 ng/mL G3P in MeOH were prepared to investigate how the peak height changed over several days. Five of the replicates were analyzed on day 1, with a mean ± standard deviation (SD) peak height of 6235 ± 593. The next day, the same 5 replicates were run, in addition to another 5 replicates. The mean ± SD peak height had increased to 12436 ± 950. On day 6, all 15 replicates were analyzed. The mean ± SD was now decreased to 9376 ± 340.

4.3 Sample preparation and G3P extraction

G3P was extracted according to the procedure described in (Paynter et al., 2018), using 30 µL plasma and 4 volumes of 80 % MeOH for PPT before direct injection to the HILIC-MS system**.** No peaks were observed with *m/z* value of 171.0058. No peaks were identified using larger volumes of plasma (up to 200 µL) as well.

Different solvents, ACN, acetone, EtOH and PrOH, were tested for PPT of plasma samples. Only small peaks (not measurable) were identified when using ACN as precipitation

solvent. An experiment was set up where EtOH or ACN were used for PPT, and the supernatant evaporated at 60 ˚C after centrifugation. The solids were then resuspended in 1 % ammonium acetate in PrOH. Now there were noticeable peaks in the EtOH samples and small peaks for the ACN samples. A calibration curve (standard addition calibration) was attempted set up using 4 plasma samples spiked with G3P (0 ng/mL, 4 552 ng/mL, 9105 ng/mL, and 13 567 ng/mL G3P in the plasma samples). This time there was only observed a peak for G3P in the sample spiked with 9 105 ng/mL. A second attempt was made; however, no peaks were registered for any of the samples.

4.4 The effect of heat and acid on G3P amount in plasma

To test whether heat and/or acid influenced the amount of G3P amount in plasma samples, four samples with three replicates were prepared; group 1: No heat or acid, group 2: heat (110 ˚C), group 3: acid (5 % HCl), group 4: heat and acid. HCl was used as PTSA (*m/z* = 171.01) gave significant ion suppression. The experiment was carried out two times with two different PPT solvents, EtOH and ACN. It was not possible to measure any G3P for any of the replicates in group 1 using EtOH as PPT solvent. Visual comparison of the boxplots show that the combination of heat and acid increased the amount of measured G3P (**Figure 21**).

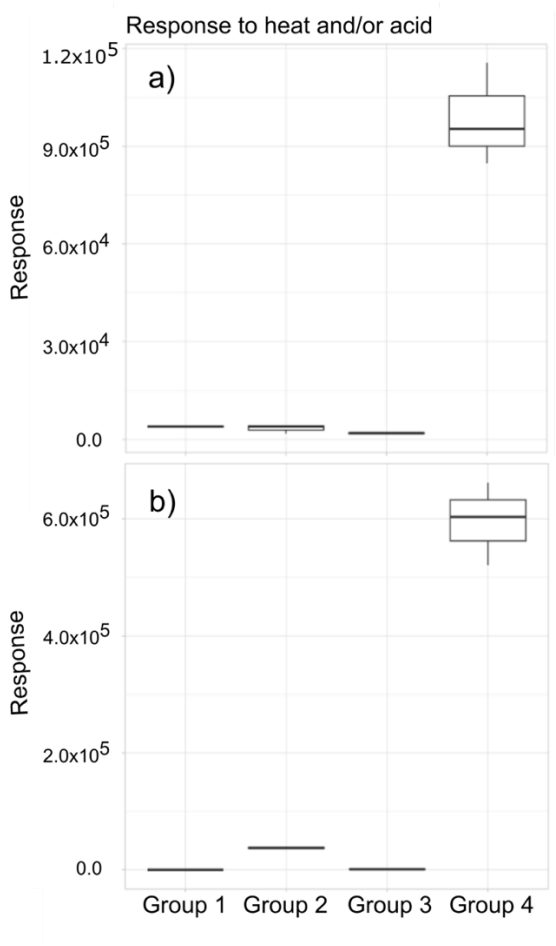

Figure 21. Difference in measured G3P amount between samples treated with or without heat (110 ˚C) and/or acid (HCl). Group 1: neither heat or acid. Group 2: heat. Group 3: acid. Group 4: heat and acid. A) ACN used as PPT solvent b) EtOH used as PPT solvent.

5 Discussion

5.1 Derivatization

Derivatization of G3P with 9FlMe was accomplished as indicated by the correct *m/z* value in the mass spectrum. However, the yield was low and difficult to track with HPLC-F, as the peak was a mix of the diester product and potential biproducts. Derivatization in plasma or serum was never attempted, as the number of biproduct was assumed to be even higher. Further, it was difficult to determine if the excitation and emission wavelengths were optimal for the G3P 9FlMe diester product. The solubility of G3P in ACN was poor, which may have contributed to the low yield. G3P readily dissolves in protic solvents like water and alcohols, but these couldn't be used in the esterification reaction. A possible approach could involve employing an alcohol derivatization reagent that serves both as a reaction solvent and a derivatization reagent. 2-phenylethanol is such a potential reagent. It is a liquid alcohol that contains a chromophore, which enables its detection through UV-Vis spectroscopy.

Derivatization of G3P in plasma with BuOH was successful with the diester being formed here as well. This product was easier to identify compared to G3P 9FlMe, as the MS is selective for a certain *m/z* ratio. This reaction was carried out using G3P spiked serum spiked and gave promising results. However, the variability in the measured concentration was high between replicate samples.

5.2 HILIC

Analyzing G3P using HILIC-MS had already been reported (Chiles et al., 2019; Paynter et al., 2018), although there was no record of any measured concentration. In this experiment, an Acquity BEH amide column was able to retain G3P dissolved in water/ACN or alcohols (MeOH, EtOH and PrOH). Since plasma and serum samples contain a considerable amount of water, this water needed to be evaporated before sample injection onto the HILIC column, preventing peak splitting. Experimentation with evaporation and redissolution gave highly variable or no peaks at all for G3P spiked serum. This could perhaps be due to the high salt concentration in the injected sample, as it was shown that a high salt content (4 %) decreased peak height compared to 1 % salt. Further, there was a high variability in peak height for replicate samples analyzed at two succeeding days. Consequently, it was difficult to interpret how changing the mobile phase composition influenced the sensitivity of the method. The reason for the high variability was not discovered.

5.3 Phospholipid hydrolysis

An experiment was set up where the G3P amount was compared in samples exposed to heat and/or acid and samples unexposed. The samples exposed to heat and acid showed higher amounts of G3P compared to the other groups. This indicates that there had been a formation of G3P, possibly through hydrolysis of phosphatidylglycerol, or other phospholipids, which were not excluded through PPT (**Figure 22**). The samples where EtOH was used as PPT solvent yielded a higher amount of G3P. Phospholipids are generally more soluble in alcohols than ACN (Alzweiri et al., 2008). Consequently, using an alcohol as PPT solvent in plasma generally yields more phospholipids in the supernatant. This would explain the higher amount of G3P in the sample where EtOH had been used for PPT, and a higher formation of G3P butyl diesters where MeOH was used for PPT.

A potential solution to the phospholipid hydrolysis problem could be to separate the phospholipids from the rest of the sample, through application of either LLE or SPE during sample preparation. RP-SPE would retain phospholipids due to the hydrophobic fatty chains. Alternatively, addition of nonpolar solvents to plasma should extract the phospholipids into the organic phase. Further research could explore these possibilities.

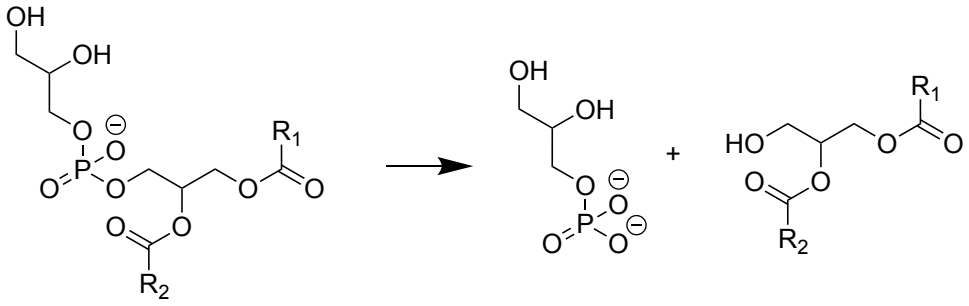

Figure 22. Possible hydrolysis of phosphatidylglycerol when exposed to heat and acid leading to an increased G3P amount in plasma.

5.4 Conclusion

G3P was derivatized through an esterification reaction with alcohols, 9FlMe and BuOH in this research. The reaction utilized heat and an acid catalyst to speed up the process, which may have contributed to an exaggerated G3P amount in plasma and serum samples due to phospholipid hydrolysis. Phospholipids should be excluded from the sample before derivatization, which could possibly be achieved through either LLE or SPE. This must be further investigated. Analyzing G3P directly using a HILIC column was possible, although there was a high variability in peak height from identical replicates analyzed on different days.

References

Abbott, S. R. (1980). Practical aspects of normal-phase chromatography. *Journal of chromatographic science, 18*(10), 540-550. https://doi.org/10.1093/chromsci/18.10.540

Abcam. (2023, 10. August). Glycerol-3-phosphate (G3P) Assay Kit (Colorimetric) (ab174094). Retrieved from https://www.abcam.com/products/assay-kits/glycerol-3-phosphate-g3p-assay-kit-colorimetric-ab174094.html

Alaini, A., Malhotra, D., Rondon-Berrios, H., Argyropoulos, C. P., Khitan, Z. J., Raj, D. S. C., Rohrscheib, M., Shapiro, J. I., & Tzamaloukas, A. H. (2017). Establishing the presence or absence of chronic kidney disease: Uses and limitations of formulas estimating the glomerular filtration rate. *World J Methodol, 7*(3), 73-92. https://doi.org/10.5662/wjm.v7.i3.73

Alpert, A. J. (1990). Hydrophilic-interaction chromatography for the separation of peptides, nucleic acids and other polar compounds. *Journal of chromatography A, 499*, 177-196. https://doi.org/10.1016/S0021-9673(00)96972-3

Alzweiri, M., Watson, D. G., Robertson, C., Sills, G. J., & Parkinson, J. A. (2008). Comparison of different water-miscible solvents for the preparation of plasma and urine samples in metabolic profiling studies. *Talanta, 74*(4), 1060-1065. https://doi.org/10.1016/j.talanta.2007.07.037

Bachmann, L. M., & Miller, W. G. (2020). Chapter 7 - Spectrophotometry. In W. Clarke & M. A. Marzinke (Eds.), *Contemporary Practice in Clinical Chemistry (Fourth Edition)* (pp. 119-133): Academic Press.

Banfi, G., Salvagno, G. L., & Lippi, G. (2007). The role of ethylenediamine tetraacetic acid (EDTA) as in vitro anticoagulant for diagnostic purposes. *Clin Chem Lab Med, 45*(5), 565-576. https://doi.org/10.1515/cclm.2007.110

Bank, R. A., Jansen, E. J., Beekman, B., & te Koppele, J. M. (1996). Amino acid analysis by reverse-phase high-performance liquid chromatography: improved derivatization and detection conditions with 9-fluorenylmethyl chloroformate. *Analytical biochemistry, 240*(2), 167-176. https://doi.org/10.1006/abio.1996.0346

Bezerra, M. A., dos Santos, Q. O., Santos, A. G., Novaes, C. G., Ferreira, S. L. C., & de Souza, V. S. (2016). Simplex optimization: a tutorial approach and recent applications in analytical chemistry. *Microchemical Journal, 124*, 45-54. http://dx.doi.org/10.1016/j.microc.2015.07.023

Blanchard, J. (1981). Evaluation of the relative efficacy of various techniques for deproteinizing plasma samples prior to high-performance liquid chromatographic analysis. *Journal of Chromatography B: Biomedical Sciences and Applications, 226*(2), 455-460. https://doi.org/10.1016/s0378-4347(00)86080-6

Bruker. (2014). impact series User Manual. In. Billerica, Massachusetts, USA: Bruker.

Cardinael, P., Casabianca, H., Peulon-Agasse, V., & Berthod, A. (2015). Sample derivatization in separation science. In J. L. Anderson, A. Berthod, V. Pino, & A. M. Stalcup (Eds.), *Analytical Separation Science* (Vol. 5). Weinheim, Germany: Wiley-VCH.

Chiles, E., Wang, Y., Kalemba, K. M., Kwon, H., Wondisford, F. E., & Su, X. (2019). Fast LC-MS quantitation of glucose and glycerol via enzymatic derivatization. *Analytical biochemistry, 575*, 40-43. https://doi.org/10.1016/j.ab.2019.03.020

Dueymes, C., Pirat, C., & Pascal, R. (2008). Facile synthesis of simple mono-alkyl phosphates from phosphoric acid and alcohols. *Tetrahedron Letters, 49*(36), 5300-5301. https://doi.org/10.1016/j.tetlet.2008.06.083

Greco, G., & Letzel, T. (2013). Main Interactions and Influences of the Chromatographic Parameters in HILIC Separations. *Journal of chromatographic science, 51*(7), 684-693. https://doi.org/10.1093/chromsci/bmt015

Hunt, D. F., Yates 3rd, J., Shabanowitz, J., Winston, S., & Hauer, C. R. (1986). Protein sequencing by tandem mass spectrometry. *Proceedings of the National Academy of Sciences, 83*(17), 6233-6237. https://doi.org/10.1073%2Fpnas.83.17.6233

Jing, C., Zhenyu, D., Qun, X., & Lina, L. (n.d). *Sensitive and rapid determination of polycyclic aromatic hydrocarbons in tap water*. Retrieved from Sunnyvale, California, USA: https://assets.thermofisher.com/TFS-Assets/CMD/Application-Notes/AN-1085-LC-PAHs-Tap-Water-AN70923-EN.pdf

Joseph, M. (n.d). *HPLC Detector Options for the Determination of Polynuclear Aromatic Hydrocarbons*. Retrieved from https://www.agilent.com/library/applications/lc07.pdf

Kaklamanos, G., Aprea, E., & Theodoridis, G. (2016). Mass Spectrometry: Principles and Instrumentation. In B. Caballero, P. M. Finglas, & F. Toldrá (Eds.), *Encyclopedia of Food and Health* (pp. 661-668). Oxford: Academic Press.

Kalantar-Zadeh, K., Jafar, T. H., Nitsch, D., Neuen, B. L., & Perkovic, V. (2021). Chronic kidney disease. *The lancet, 398*(10302), 786-802. https://doi.org/10.1016/s0140-6736(21)00519-5

Keana, J. F. W., Shimizu, M., & Jernstedt, K. K. (1986). A short, flexible route to symmetrically and unsymmetrically substituted diphosphatidylglycerols (cardiolipins).

The Journal of Organic Chemistry, 51(12), 2297-2299. https://doi.org/10.1021/jo00362a024

Khan, Z., Javed, F., Shamair, Z., Hafeez, A., Fazal, T., Aslam, A., Zimmerman, W. B., & Rehman, F. (2021). Current developments in esterification reaction: A review on process and parameters. *Journal of Industrial and Engineering Chemistry, 103*, 80-101. https://doi.org/10.1016/J.JIEC.2021.07.018

Krebs, H. A. (1950). Chemical composition of blood plasma and serum. *Annual Review of Biochemistry, 19*(1), 409-430. https://doi.org/10.1146/annurev.bi.19.070150.002205

Lee, J., & Ridgway, N. D. (2020). Substrate channeling in the glycerol-3-phosphate pathway regulates the synthesis, storage and secretion of glycerolipids. *Biochimica et Biophysica Acta (BBA)-Molecular and Cell Biology of Lipids, 1865*(1), 158438. https://doi.org/10.1016/j.bbalip.2019.03.010

Lindroth, P., & Mopper, K. (1979). High performance liquid chromatographic determination of subpicomole amounts of amino acids by precolumn fluorescence derivatization with o-phthaldialdehyde. *Analytical Chemistry, 51*(11), 1667-1674. https://doi.org/10.1021/ac50047a019

Liu, S., & Quarles, L. D. (2007). How fibroblast growth factor 23 works. *Journal of the American Society of Nephrology, 18*(6), 1637-1647. https://doi.org/10.1681/asn.2007010068

Lundanes, E., Reubsaet, L., & Greibrokk, T. (2013). *Chromatography: basic principles, sample preparations and related methods*: John Wiley & Sons

Lv, J.-C., & Zhang, L.-X. (2019). Prevalence and Disease Burden of Chronic Kidney Disease. *Advances in experimental medicine and biology, 1165*, 3-15. https://doi.org/10.1007/978-981-13-8871-2_1

Martin, A., David, V., & Quarles, L. D. (2012). Regulation and function of the FGF23/klotho endocrine pathways. *Physiological reviews*. https://doi.org/10.1152/physrev.00002.2011

McCalley, D. V. (2017). Understanding and manipulating the separation in hydrophilic interaction liquid chromatography. *Journal of chromatography A, 1523*, 49-71. http://dx.doi.org/10.1016/j.chroma.2017.06.026

Naldi, A. C., Fayad, P. B., Prévost, M., & Sauvé, S. (2016). Analysis of steroid hormones and their conjugated forms in water and urine by on-line solid-phase extraction coupled to liquid chromatography tandem mass spectrometry. *Chemistry Central Journal, 10*(1), 1-17. https://doi.org/10.1186%2Fs13065-016-0174-z

Pawula, M., Hawthorne, G., Smith, G. T., & Hill, H. M. (2013). Best Practice in Biological Sample Collection, Processing, and Storage for LC-MS in Bioanalysis of Drugs. In W. Li, J. Zhang, & F. L. S. Tse (Eds.), *Handbook of LC-MS Bioanalysis: Best Practices, Experimental Protocols, and Regulations* (pp. 139-164). Hoboken, New Jersey, USA: John Wiley & Sons.

Paynter, N. P., Balasubramanian, R., Giulianini, F., Wang, D. D., Tinker, L. F., Gopal, S., Deik, A. A., Bullock, K., Pierce, K. A., & Scott, J. (2018). Metabolic predictors of incident coronary heart disease in women. *Circulation, 137*(8), 841-853. https://doi.org/10.1161/CIRCULATIONAHA.117.029468

Poole, C. F. (2003). New trends in solid-phase extraction. *TrAC Trends in Analytical Chemistry, 22*(6), 362-373. https://doi.org/10.1016/S0165-9936(03)00605-8

Reshef, L., Olswang, Y., Cassuto, H., Blum, B., Croniger, C. M., Kalhan, S. C., Tilghman, S. M., & Hanson, R. W. (2003). Glyceroneogenesis and the triglyceride/fatty acid cycle. *Journal of Biological Chemistry, 278*(33), 30413-30416. https://doi.org/10.1074/jbc.r300017200

Santa, T. (2013). Derivatization in LC-MS Bioanalysis. In Wenkui Li, Jie Zhang, & F. L. S. Tse (Eds.), *Handbook of LC-MS Bioanalysis: Best Practices, Experimental Protocols, and Regulations.* (pp. 239-248): John Wiley & Sons.

Shimadzu. (2023a, 10. August). Fluorescence Detection. Retrieved from https://www.shimadzu.com/an/service-support/technical-support/analysis-basics/basic/fluorescence_detection.html

Shimadzu. (2023b, 10. August). Interfaces for LC-MS. Retrieved from https://www.shimadzu.com/an/service-support/technical-support/analysis-basics/basics_of_lcms/interfaces_for_lcms.html#section1

Shimadzu. (2023c, 10. August). Introduction to mass analyzers. Retrieved from https://www.shimadzu.com/an/service-support/technical-support/analysis-basics/fundamental/mass_analyzers.html

Simic, P., Kim, W., Zhou, W., Pierce, K. A., Chang, W., Sykes, D. B., Aziz, N. B., Elmariah, S., Ngo, D., & Pajevic, P. D. (2020). Glycerol-3-phosphate is an FGF23 regulator derived from the injured kidney. *The Journal of Clinical Investigation, 130*(3), 1513-1526. https://doi.org/10.1172/JCI131190

Skoog, D. A., Holler, F. J., & Crouch, S. R. (2018). *Principles of Instrumental Analysis, Seventh Edition*: Cengage Learning

Snyder, L. R., Kirkland, J. J., & Dolan, J. W. (2010). *Introduction to modern liquid chromatography*: John Wiley & Sons

Soderberg, T. (2019). *Organic Chemistry with a Biological Emphasis Volume II*: Chemistry Publications. https://digitalcommons.morris.umn.edu/chem_facpubs/2

Takeuchi, T. (2005). HPLC of amino acids as dansyl and dabsyl derivatives. In *Journal of Chromatography Library* (Vol. 70, pp. 229-241): Elsevier.

Thorner, J. W., & Paulus, H. (1973). The Enzymes. In P. D. Boyer (Ed.), (Vol. 8, pp. 487-494): Academic Press.

Tijburg, L. B. M., Geelen, M. J. H., & van Golde, L. M. G. (1989). Regulation of the biosynthesis of triacylglycerol, phosphatidylcholine and phosphatidylethanolamine in the liver. *Biochimica et Biophysica Acta (BBA) - Lipids and Lipid Metabolism, 1004*(1), 1-19. https://doi.org/10.1016/0005-2760(89)90206-3

Wahl, P., & Wolf, M. (2012). FGF23 in chronic kidney disease. *Endocrine FGFs and Klothos*, 107-125. https://doi.org/10.1007/978-1-4614-0887-1_8

Waters. (2023, 10. August). Columns. Retrieved from https://www.waters.com/nextgen/no/en/products/columns.html

Williams, J. R., & Boehm, J. C. (1995). Studies on the synthesis of dehydroepiandrosterone (DHEA) phosphatide. *Steroids, 60*(4), 333-336. https://doi.org/10.1016/0039-128x(95)00003-9

Yoshitake, T., Kehr, J., Todoroki, K., Nohta, H., & Yamaguchi, M. (2005). Derivatization chemistries for determination of serotonin, norepinephrine and dopamine in brain microdialysis samples by liquid chromatography with fluorescence detection. *Biomedical Chromatography, 20*(3), 267-281. https://doi.org/10.1002/bmc.560

Appendix I

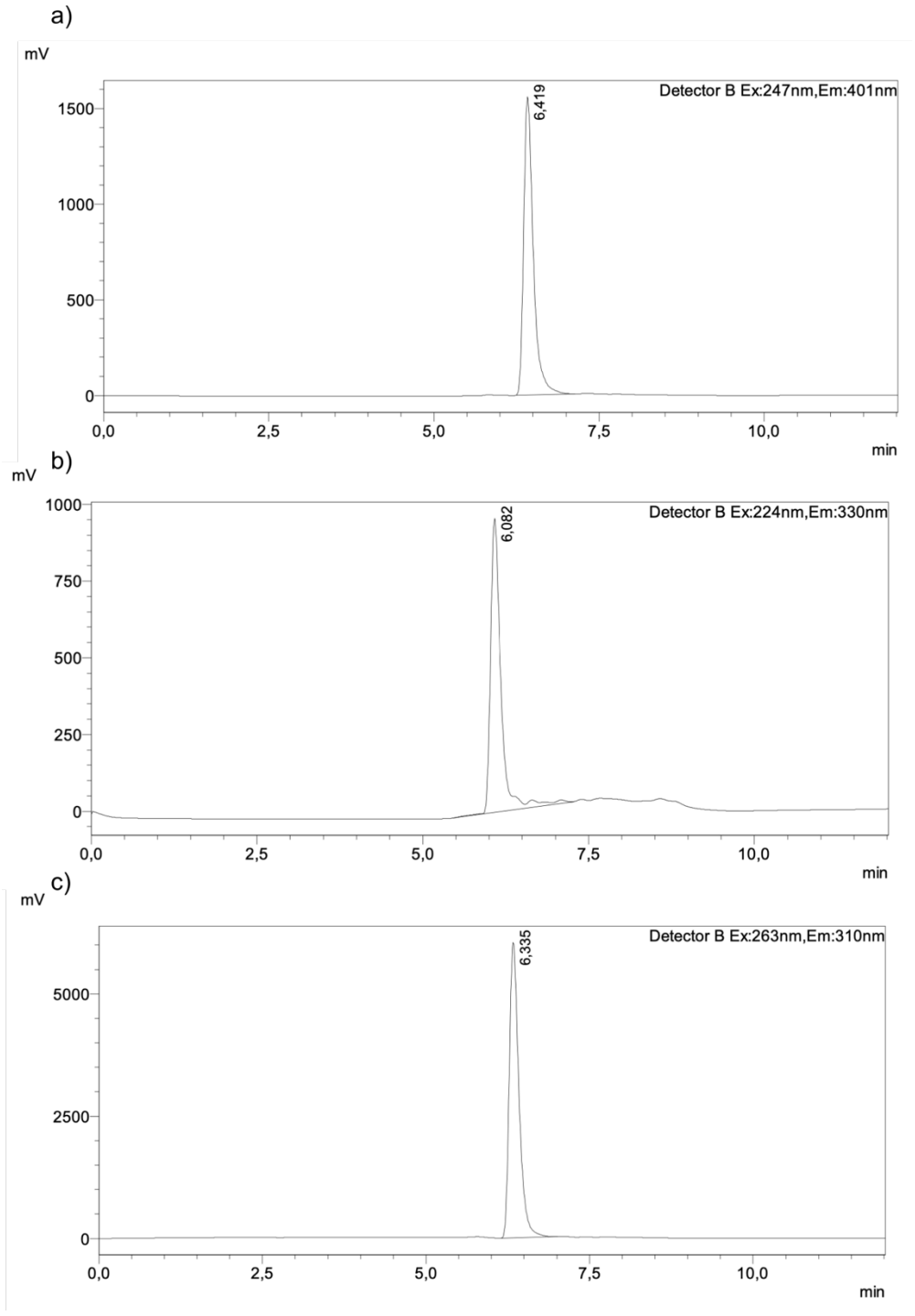

Figure I-23. Chromatograms of fluorescent derivatization reagents. A) 9AnMe b) 1NaMe and c) 9FlMe.

Appendix II

Table II-9. Results from G3P derivatization with BuOH to G3P butyl diesters. G3P-AN0 to G3P-AN3 were used to set up a calibration curve for estimation of G3P butyl diester concentrations. Response is the area divided by the IS area.

ID	Type	Std. Conc	RT	Area	IS Area	Response	µmol/l
STD 0	Blank		1.78	5870	8467	0.693	2.855
STD 0	Blank		1.78	5080	7425	0.684	2.817
STD 1	Analyte		1.78	3160	11725	0.270	1.110
STD 2	Analyte		1.78	3560	13305	0.268	1.102
STD 3	Analyte		1.78	2109	10270	0.205	0.846
STD 4	Analyte		1.78	7004	12247	0.572	2.355
STD 5	Analyte		1.78	35576	15642	2.274	9.365
STD 6	Analyte		1.78	17574	14660	1.199	4.937
PBS	Blank		1.78	29291	8954	3.271	13.471
PBS	Blank		1.78	30953	9206	3.362	13.845
99999567	Analyte		1.78	273848	15962	17.156	70.647
99999566	Analyte		1.78	443451	34026	13.033	53.667
99999567	Analyte		1.78	710121	29876	23.769	97.877
G3P-AN0	Standard	60.207	1.78	401748	27309	14.711	60.581
G3P-AN1	Standard	160.207	1.78	853630	22051	38.711	159.409
G3P-AN2	Standard	260.207	1.78	1618622	25638	63.133	259.977
G3P-AN3	Standard	360.207	1.78	2352948	26908	87.443	360.083
G3Pstd	Analyte	28.900	1.78	253761	29501	8.602	35.421
99999566	Analyte		1.78	298537	10279	29.042	119.593

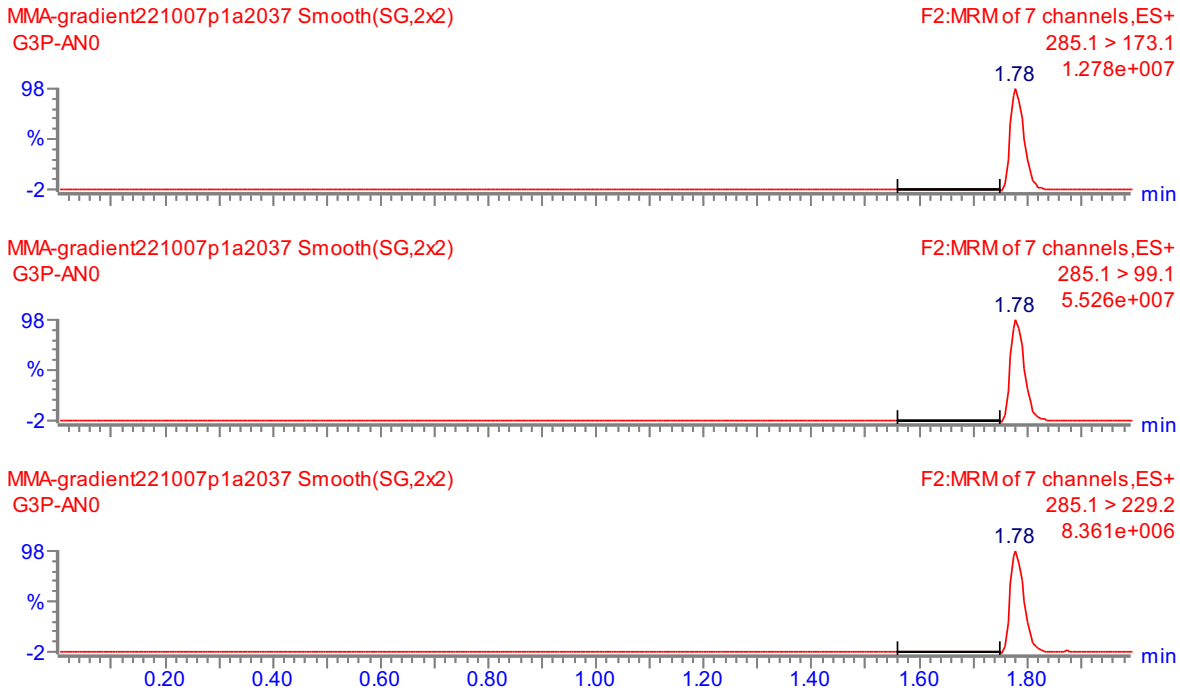

Figure II-24. Chromatograms of G3P butyl diesters analyzed with LC-MS/MS.